Chapter 13:Permian–Triassic felsic tuffs in South Island, New Zealand: significance for oceanic and active continental margin subduction

Chapter 11

Geochemistry used to infer source characteristics and provenance of mudrocks of the Permian–Triassic Maitai Group and the associated Patuki Melange, South Island, New Zealand

ROMESH PALAMAKUMBURA* & ALASTAIR H. F. ROBERTSON

School of GeoSciences, University of Edinburgh, Grant Institute, James Hutton Road, Edinburgh EH9 3FE, UK

R.P., 0000-0002-6863-6916

**Correspondence:* *romesh@bgs.ac.uk*

Abstract: Chemical and mineralogical evidence is reported, first for mudrocks from the Mid-Permian–Mid-Triassic Maitai Group and, secondly, for Late Permian(?) mudrocks from the structurally underlying Patuki Melange. Weathering and alteration indices indicate increased source weathering and aluminosilicate input stratigraphically upwards in the Maitai Group. The Maitai Group exhibits an upward change from a relatively enriched continental magmatic arc source (and related country rocks) during the Late Permian, to a relatively depleted continental magmatic arc source (and related country rocks) during the Triassic. The melange mudrocks have a similar provenance to the Late Permian mudrocks of the Maitai Group. The melange mudrocks are, however, generally less altered, probably because of additional, local, ophiolite-related input. Red iron-rich mudrocks accumulated widely in two Triassic Maitai Group formations and also locally in the Patuki Melange. The iron oxide was derived by continental weathering under warm conditions, and then accumulated relatively slowly under oxidizing seafloor conditions. The chemical evidence, as a whole, indicates sources for all of the mudrocks similar to the Median Batholith and associated country rocks, or non-exposed equivalents along the SE Gondwana active continental margin. Accumulation took place during a change from an icehouse to a hothouse world.

Supplementary material: Geochemical data are available at https://doi.org/10.6084/m9.figshare.c.4397687

The chemical composition of mudrocks, especially in well-constrained geological settings, is a powerful indication of source constituents and provenance (Bhatia 1985; Roser & Korsch 1986, 1988; McLennan *et al.* 1993; Armstrong-Altrin 2015). However, the tendency of, in particular, major elements to be affected by sediment transport, diagenesis, metamorphism or weathering can impose limitations on interpretation (e.g. Roser & Korsch 1986, 1988; Wronkiewicz & Condie 1987; McLennan 1989; Cox *et al.* 1995; Lee 2002; Ejeh 2016). Relatively stable elements are, therefore, favoured for provenance analysis of mudrocks (e.g. Hassan *et al.* 1999; Cullers 2000; Long *et al.* 2008; Paikaray *et al.* 2008). Interpretation is most effective when several techniques are combined, including mineralogical analysis (Herron 1988; Cavalcante *et al.* 2003), isotopic analysis (e.g. Bock *et al.* 1994), electron microscopy (e.g. Ahn *et al.* 1988) and detrital element geochronology (e.g. Yang *et al.* 2012).

In New Zealand, geochemical studies of clastic sedimentary sequences of Permian and Triassic age have mainly utilized sandstones (Roser & Korsch 1986, 1988; Robertson & Palamakumbura 2019*b*). Here, we focus instead on mudrocks (grain size <0.062 mm) from two different components of the key regionally developed Dun Mountain–Maitai Terrane (Fig. 11.1). The Dun Mountain–Maitai Terrane is one of several major lithostratigraphic terranes making up the Eastern Province of South Island (Mortimer *et al.* 2014; see Robertson *et al.* 2019*b*) (Fig. 11.1). The first unit studied is the Maitai Group, a coherent succession, up to *c.* 6000 m thick, which is dated as Mid-Permian–Mid-Triassic in age (Waterhouse 1959, 1964, 1980; Aitchison *et al.* 1988; Aitchison & Landis 1990; Owen 1995; Campbell 2000; Krull *et al.* 2000; Stratford *et al.* 2004; Campbell 2019) (Fig. 11.1). The Maitai Group is widely (but not exclusively) interpreted as a continental margin forearc basin adjacent to SE Gondwana (Owen 1995; Robertson & Palamakumbura 2019*b*). The second unit studied is the Patuki Melange, which underlies the Dun Mountain ophiolite and is interpreted as accretionary melange related to the westward subduction of Panthalassa oceanic lithosphere beneath SE Gondwana (Jugum 2009; Jugum *et al.* 2019; Robertson 2019*a*, *b*). The Patuki Melange was chosen to test the interpretation, based on sandstone chemistry (Robertson & Palamakumbura 2019*b*), that the provenance of the Patuki Melange is similar to the Late Permian sandstones of the Wooded Peak Formation and/or the Tramway Formation of the Maitai Group. In addition, both the Maitai Group and the Patuki Melange include distinctive reddish coloured shales of debatable origin.

We begin by summarizing the sedimentology of the mudrocks in both units, and then present and interpret our new geochemical evidence, supported by semi-quantitative X-ray diffraction (XRD). We use the timescale of Raine *et al.* (2015), as correlated with the international timescale (Gradstein *et al.* 2012).

In provenance studies, differing clast or grain sizes can yield different types of information (e.g. Miall 2013). Conglomerates tend to provide information on specific sources, locations, or geological events: for example, derivation from a topographically rugged or faulted source area. Sandstones typically provide information on a wider source region, but mostly restricted to specific depositional pathways and depocentres. In contrast, muds are capable of being carried long distances by rivers, wind, gravity flows or ocean currents. Mud and mudrock chemistry can, therefore, indicate large-scale or long-term variations and trends in provenance, which may be less easily recognizable in coarser-grained deposits.

The Dun Mountain–Maitai Terrane encompasses three different components. The first is the Dun Mountain ophiolite and related oceanic arc rocks (Otama Complex), which comprises oceanic lithosphere of late Early Permian (*c.* 278–269 Ma) age (Jugum 2009; Jugum *et al.* 2019) that is interpreted, based on petrological and geochemical evidence, to have formed above a subduction zone (Coombs *et al.* 1976; Davis *et al.* 1980; Sinton 1980; Kimbrough *et al.* 1992; Sivell & McCulloch 2000; Jugum 2009; Jugum *et al.* 2019). The second unit

From: Robertson, A. H. F. (ed.) 2019. *Paleozoic–Mesozoic Geology of South Island, New Zealand: Subduction-related Processes Adjacent to SE Gondwana*. Geological Society, London, Memoirs, **49**, 267–285, https://doi.org/10.1144/M49.13

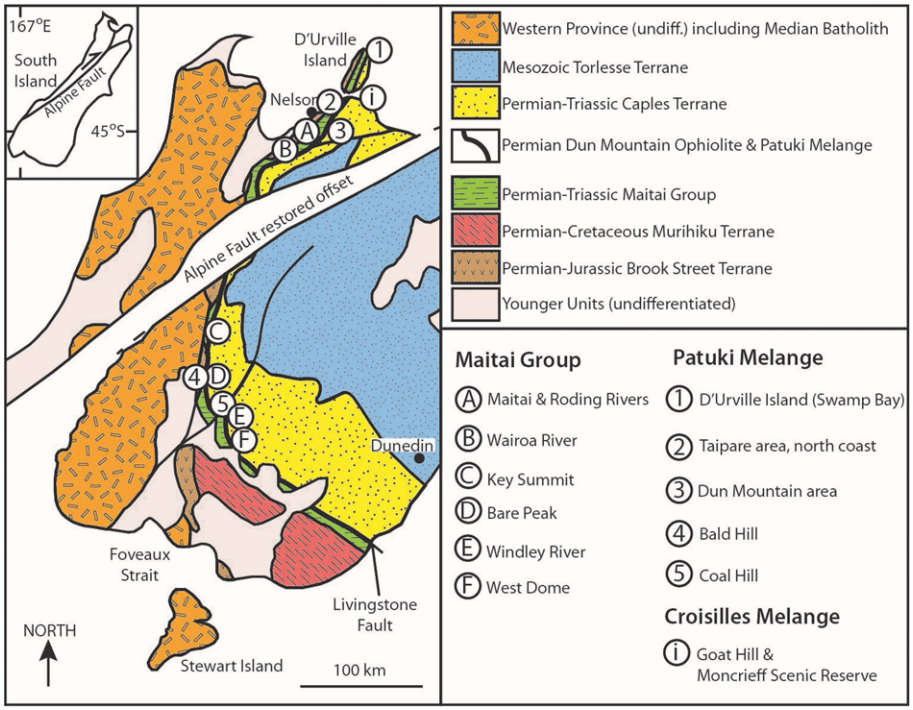

Fig. 11.1. Outline tectonic map of South Island showing the locations and geological units of the mudrocks sampled for geochemical and XRD analysis from the Maitai Group overlying the Dun Mountain ophiolite and from the Patuki Melange beneath the ophiolite, restored to their approximate positions before Neogene–Quaternary offset by the Alpine Fault. One locality of the Croisilles Melange is also shown, for comparison. Outline geology based on Mortimer *et al.* (1999).

is the sedimentary cover of the ophiolite, represented by the Mid-Permian–Mid-Triassic Maitai Group (Landis 1969, 1974, 1980; Owen 1995; Stratford *et al.* 2004; Robertson & Palamakumbura 2019*b*, *c*). The third component is the Patuki Melange, which is named after its type area on D'Urville Island (Johnston 1981, 1982; Cawood 1986, 1987; Landis & Blake 1987; Begg & Johnston 2000; Sivell 2002; Jugum *et al.* 2019; Robertson 2019*a*) (Fig. 11.1). Outcrops to the south of the Alpine Fault were originally given different names (Coombs *et al.* 1976; Craw 1979) but have since been correlated with the Patuki Melange (Turnbull 2000; Turnbull & Allibone 2003; Robertson 2019*a*).

The Patuki Melange is dominated by dismembered thrust slices and blocks of sandstone–shale, together with mainly ophiolite-related ultramafic rocks (serpentinized), basic to felsic intrusive rocks and basaltic extrusive rocks (Rattenbury *et al.* 1998; Sivell & McCulloch 2000; Begg & Johnston 2000; Sivell 2002; Robertson 2019*a*). Limited available biostratigraphic evidence suggests that the shales and sandstones within the melange are Late Permian in age, based mainly on the presence of atomodesmatinid bivalve shell fragments (Dickins *et al.* 1986; Rattenbury *et al.* 1998).

The specific objectives of this study are: (1) to compare the chemical composition and provenance of the mudrocks of the Maitai Group and the Patuki Melange, with implications for plate tectonic reconstruction; (2) to determine the degree of weathering and alteration affecting both units; and (3) to identify and interpret any long-term changes in the provenance, tectonic setting, or climate represented by the Maitai Group. The study uses mudrock samples from seven outcrops of the Maitai Group and six outcrops of the Patuki Melange (Fig. 11.1).

Sedimentology of the mudrocks

The Maitai Group can be subdivided into a lower part comprising the Upukerora, Wooded Peak and Tramway formations of Permian age, which are dominated by variable mixtures of volcaniclastic and/or terrigenous sediments. Above this, the upper part of the succession comprises the Little Ben Formation, the Greville Formation, the Waiua Formation and the Stephens Subgroup (up to six formations) of mainly Early–Mid-Triassic age, all of which are predominantly volcaniclastic (Fig. 11.2). The Little Ben Formation is likely to straddle the Permian–Triassic boundary (Campbell 2019). Tuffaceous sediments that are locally abundant in the Triassic formations are discussed by Robertson *et al.* (2019*c*).

The term mudrocks is used here to encompass mudstones (which are blocky and non-fissile), shales (which are finely laminated or fissile), argillite (which is relatively indurated), slate (which is cleaved), siltstone, claystone and marl (Tucker 1991). In practice, many of the mudrocks studied are shales. An attempt was made to collect mudrocks of similar grain size. Marls occur in certain parts of the succession, whereas claystones are rare. Tuffs were excluded.

Mudrocks have two main modes of occurrence throughout the Maitai Group (Fig. 11.3). First, they occur as discrete interbeds (Fig. 11.3a), ranging from centimetres, to tens of centimetres, to, occasionally, metres in thickness, at different levels in the overall sequence. These sediments range from massive (Fig. 11.3d, e), to planar laminated (Fig. 11.3b), and vary from non-bioturbated (Fig. 11.3b) to bioturbated (Fig. 11.3i). Secondly, mudrocks also occur in the upper parts of individual gravity-flow deposits, specifically as the D and E divisions of classical turbidites (Bouma 1962). These mudrock intervals are typically thin (<5 cm), silty and normal-graded (Fig. 11.3c, f).

Mudrocks vary considerably from formation to formation within the Maitai Group. In most formations, the mudrocks are typically a greyish colour (brownish where weathered) (Fig. 11.3c). However, some mudrocks are dark and organic-rich, with a fetid smell, especially in the Wooded Peak Formation (Fig. 11.3a). In contrast, reddish, strongly bioturbated mudrocks characterize the Waiua and Cerberus formations (Stephens Subgroup) (Fig. 11.3f, h). Some of mudrocks show evidence of current reworking (Fig. 11.3d), deposition from low-density turbidity currents or contour currents (Fig. 11.3g), especially in the Tramway and Cerberus formations.

Mudrocks are generally absent from the basal Upukerora Formation, which is dominated by breccia-conglomerate, although silty and/or tuffaceous mudstones occur locally, mainly in the higher levels of the succession (Pillai 1989; Robertson 2019*b*). One sample of mudrock was studied from north

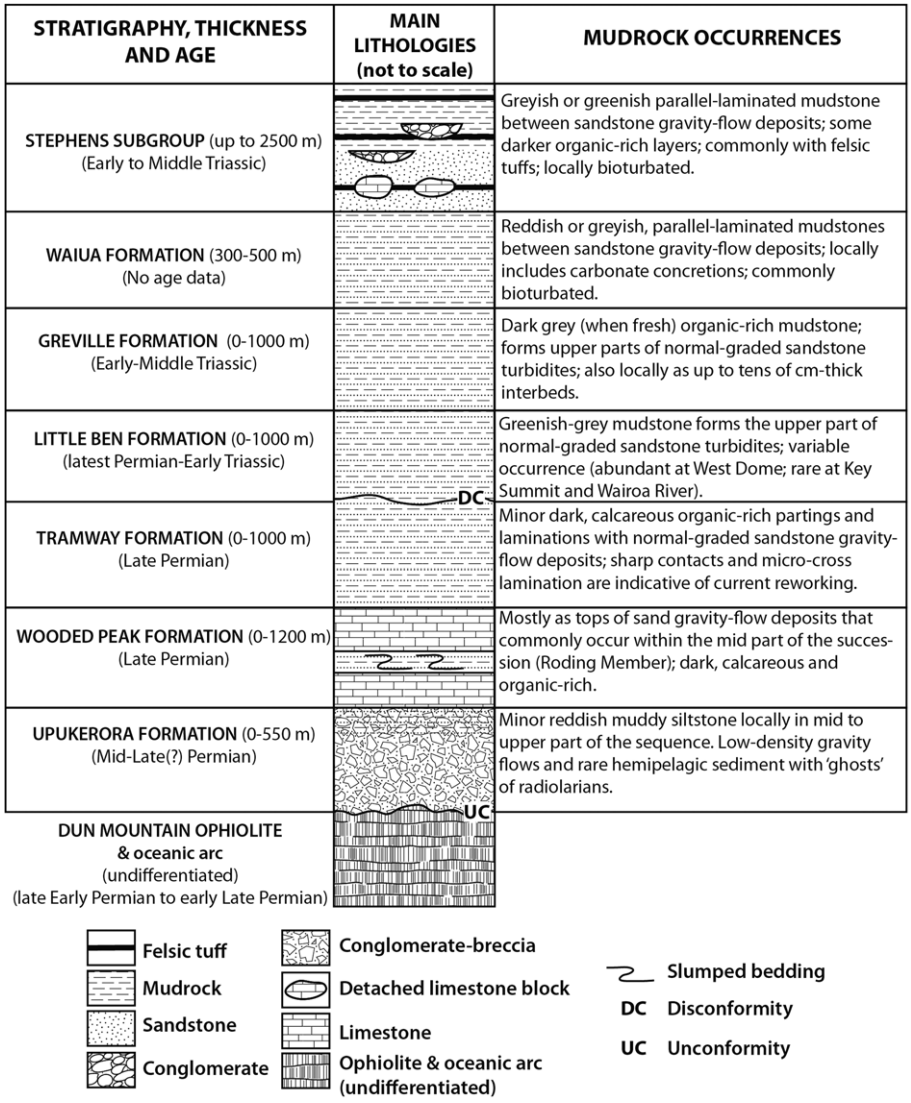

Fig. 11.2. Summary of the age and occurrence of mudrocks within the Mid-Permian–Mid-Triassic Maitai Group. Stratigraphy modified from Landis (1974), Kimbrough *et al.* (1992) and Owen (1995). The facies and thicknesses of units vary considerably on a regional scale, and some formations and members are restricted to specific areas. Units sampled: Upukerora Formation from the Windley River area; Wooded Peak Formation from Maitai River and West Dome (Waiteramea Member); Tramway Formation from Maitai River and West Dome; Little Ben Formation from Key Summit and Wairoa River; Greville Formation from Maitai River and Roding River; Waiua Formation from Roding River; Stephens Subgroup from Bare Peak (see Fig. 11.1).

of the Windley River in Southland. For the Wooded Peak Formation, samples were analysed from calcareous mudstone in the lower part of the succession and from the sandstone-rich uppermost part of the succession at West Dome, in Southland (Waitaramea Member of Stratford *et al.* 2004). Samples of the overlying Tramway Formation were studied from West Dome, the Wairoa River (Richmond area) and Key Summit ((Hollyford–Eglinton area): Landis 1980). A sample of silty mudrock was studied from the Little Ben Formation at Key Summit. Samples of the Greville Formation were studied from the Maitai, Roding and Wairoa rivers (Nelson–Richmond area). Mudrocks from the Waiua Formation are from the Roding River in the Nelson area. In addition, mudrock samples were studied from the overlying Stephens Subgroup, from the Eldon Formation, the Cerberus Formation and the Acheron Lakes Formation, all from near Bare Peak (NE Southland). A sample was included from the Cerberus Formation in the Lee River (Richmond area). An additional (less well dated) sample from the Stephens Subgroup was analysed from Mossburn Quarry (Southland).

Three contrasting settings of mudrocks in the Patuki Melange were investigated during this study.

The first setting is represented by mudrocks that are spatially or depositionally associated with basaltic rocks, in three areas, as follows: (1) associated with alkaline (ocean island-type: OIB) pillow basalt at Swamp Bay in the far north of D'Urville Island. Red mudstones that depositionally overlie the alkaline basalts in the same area were studied for comparison (Figs 11.3j & 11.4a); (2) intercalations (several metres thick) of pinkish coloured, fine-grained siliceous sedimentary rock from within subduction-influenced basaltic breccia at Taipare Bay on the north coast (Fig. 11.4b); (3) silty mudstone from a volcaniclastic sequence that depositionally overlies subduction-influenced basalts within the Coal Hill Inclusion, a kilometre-scale volcanic–sedimentary body within the melange in northern Southland (Fig. 11.4e).

The second setting is represented by mudrocks which form part of a coherent sequence of mixed terrigenous–volcaniclastic gravity-flow deposits (without any preserved sedimentary relationship with volcanic rocks). The succession studied at Bald Hill (NE Southland) begins with reddish laminated mudrocks, which were sampled, and passes upwards into sandstone, mudrock and minor conglomerate, up to *c.* 80 m thick (Fig. 11.4d).

The third type of setting is represented by grey to dark-grey, finely laminated mudrock (brown-weathering) that commonly occurs as blocks or small thrust sheets within the melange. This material is, in places, intensely indurated to form very hard argillite, locally known as pakohe (Johnston 2011). Samples of this lithology were studied from the Swamp Bay area (D'Urville Island: Fig. 11.4a) and Dun Mountain area (Fig. 11.4c). Further details of all of the above exposures are given by Robertson (2019*a*).

Most of the lithologies studied from both the Maitai Group and the melange have undergone regional greenschist-facies metamorphism. However, samples from the south

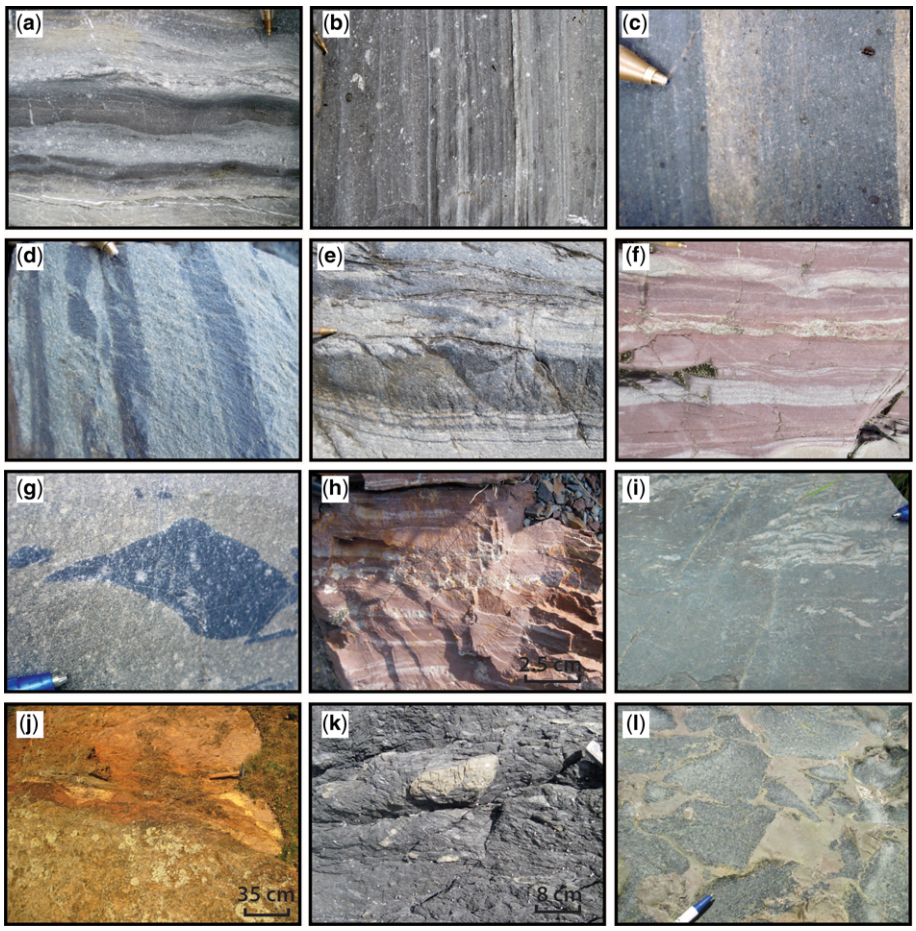

Fig. 11.3. Field photographs illustrating the sedimentology of mudrocks in the Maitai Group and the Patuki Melange. (**a**) Dark organic-rich calcareous mudrock with thin interbeds and partings, within fine- to medium-grained quartzo-feldspathic sandstone and siltstone (gravity-flow deposits); the wavy bedding is due to soft-sediment deformation, which has also resulted in localized sand injection (lower left), Roding Member, Wooded Peak Formation, Roding River (Nelson area) (note: the bedding is subvertical); the pen is for scale. (**b**) Finely-laminated calcareous mudrock (dark) with quartzo-feldspathic siltstone and fine-grained sandstone partings; the white granules are atomodesmatinid bivalve shell fragments; Roding Member, Wooded Peak Formation, Roding River; the pen is for scale. (**c**) Calcareous mudrock (dark) intercalated with thin interbeds of normal-graded quartzo-feldspathic sandstone and siltstone (gravity-flow deposits); younging to the right; near the base of the Tramway Formation, Roding River; the pen is for scale. (**d**) Thin interbeds of dark silty mudrock within fine- to medium-grained quartzo-feldspathic sandstone (younging to the right). Partial erosion of one mudrock layer is attributed to bottom-current activity; Tramway Formation, Roding River; the pen is for scale. (**e**) Dark organic-rich mudrock interbeds and partings, within fine- to medium-grained quartzose sandstone; Greville Formation, Roding River. (**f**) Red mudrock with thin interbeds of normal-graded and micro-cross-laminated sandstone–siltstone; Waiua Formation, Roding River. (**g**) Dark-coloured mudstone rip-up clast within medium-grained volcaniclastic sandstone (gravity flow), Acheron Lakes Formation, Wairoa River, Richmond area. (**h**) Red ferruginous mudrock with thin normal-graded interbeds and partings of fine-grained sandstone–siltstone, Cerberus Formation, Bare Peak, Southland. (**i**) Silty mudstone with fine tuffaceous sandstone (pale coloured; affected by burrowing); Chrome Creek Formation, Lee River, Richmond area; the pen tip (top right) is for scale. (**j**) Iron-rich mudstone depositionally overlying alkali basalt, Swamp Bay, D'Urville Island; Patuki Melange-type area. (**k**) Sheared dark, organic-rich mudrock with small phacoids of fine- to medium-grained sandstone turbidites (pale green). The phacoidal fabric is due to intense layer-parallel extension which is typical of the Patuki Melange; Swamp Bay, D'Urville Island. (**l**) Iron-rich siliceous mudrock forming the matrix of (primary) basaltic lava breccia; Patuki Melange, Taipare Bay; the pen is for scale.

(West Dome area) experienced lower-grade phrenite–pumpellyite metamorphism (Landis 1969, 1974; Coombs *et al.* 1976; Cawood 1986, 1987; Paull *et al.* 1996).

Analytical methods

Major and trace elements were analysed by X-ray fluorescence (XRF) at the School of GeoSciences, University of Edinburgh using the method detailed by Fitton *et al.* (1998). In addition, rare earth elements (REEs) were analysed at ACME Laboratories, Vancouver (Canada). Trace elements (including REEs) were determined from a $LiBO_2$ fusion by ICP-MS (inductively coupled plasma mass spectrometry) by using 5 g of sample pulp. The data are recorded together within lithology and location details in the Supplementary material.

A small suite of mudrocks from the Maitai Group and the Patuki Melange was also studied by X-ray diffraction (XRF), using the semi-quantitative method of Cusker *et al.* (1999). Data are accurate to the level of several per cent only and values <1% are not reported (see the Supplementary material).

Results

Semi-quantitative XRD results are listed in the Supplementary material, together with major and trace element data, analysed by XRF for the Maitai Group (22 samples) and the Patuki Melange (18 samples). Trace element and REE data, analysed by ICP-MS, are listed for the Maitai Group (26 samples) and for the Patuki Melange (six samples) are also given in the Supplementary material. In addition, a small amount of major

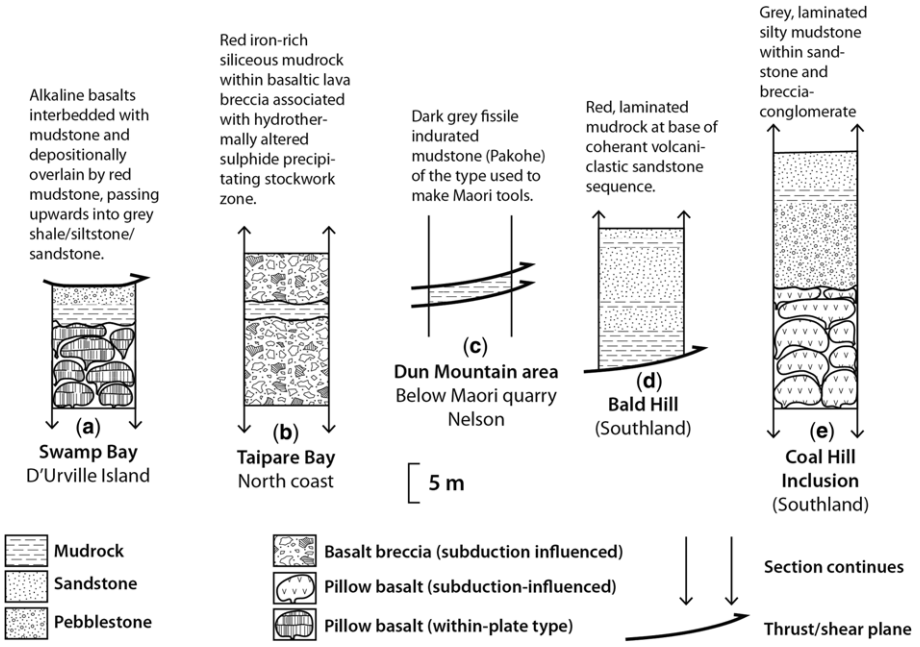

Fig. 11.4. Stratigraphical settings of the chemically analysed mudrocks from the Patuki Melange. The logs indicate the local field relationships. See Figure 11.1 for the locations.

element, trace element and REE data are included for the Croisilles Melange (see the Supplementary material; see also Robertson 2019*a*).

Semi-quantitative XRD analysis

XRD: Maitai Group. For the Maitai Group, one sample was studied for each of the formations that were chemically analysed. The results are tabulated in the Supplementary material and summarized in Figure 11.5

Quartz is generally more abundant in the basal Upukerora Formation (Fig. 11.2) than in the overlying formations (25–34%). Of the feldspars, albite ranges from trace levels in the Little Ben Formation to 38% in the Tramway Formation. Calcic feldspar (detected as anorthite) is much more abundant (22%) in the Little Ben Formation compared to the other formations (1.4–4%). Microcline occurs in small amounts generally (*c.* 2%) but is minimal in the Little Ben Formation and absent in the Cerberus Formation. Orthoclase occurs in all samples at low abundances (<3%). Muscovite is present in all samples, ranging up to 13% in the Wooded Peak Formation, with the lowest values in the Little Ben Formation (<2%).

Of the clay minerals, clinochlore is present in significant amounts (>5%) in the Upukerora, Wooded Peak, Waiua and Cerberus formations, where it reaches a maximum of 17%. Chlorite llb (a relatively high-temperature form, see below) occurs in variable amounts throughout, from trace levels in the Upukerora Formation to 8% in the Waiua Formation. Illite is detected in all samples, other than the Little Ben Formation, reaching a maximum of 10% in the Wooded Peak Formation. Kaolinite ranges from <1% in the Upukerora and Cerberus formations to 11% in the Little Ben Formation. In addition, dickite, which is genetically related to kaolinite (see below), occurs in several samples at low levels (<3%). Laumontite is relatively abundant (4%) in the Upkerora Formation but in the other formations is minimal or not detected.

Several other minerals occur in minor abundance. Calcite and dolomite are minimal. Siderite is also minimal, other than in the Little Ben Formation (5%). Rutile occurs in several samples in trace amounts. Ankerite, anatase, pyrrhotite and hematite are detected in a few samples. However, hematite reaches 3% in the red-coloured Cerberus Formation. Pyrite is present in trace amounts in the samples, except the Cerberus Formation in which it is not detected. Gypsum is minimal other than in the Little Ben Formation, where it reaches 5%. Finally, lawsonite was detected in the Cerberus Formation (10%); the stratigraphically highest of the formations sampled.

XRD: Patuki Melange. The mudrock samples from the Patuki Melange are, first, the red mudrock overlying basalt on D'Urville Island (Fig. 11.4a); secondly, red mudrock from the base of the locally intact succession at Bald Hill (Fig. 11.4d);

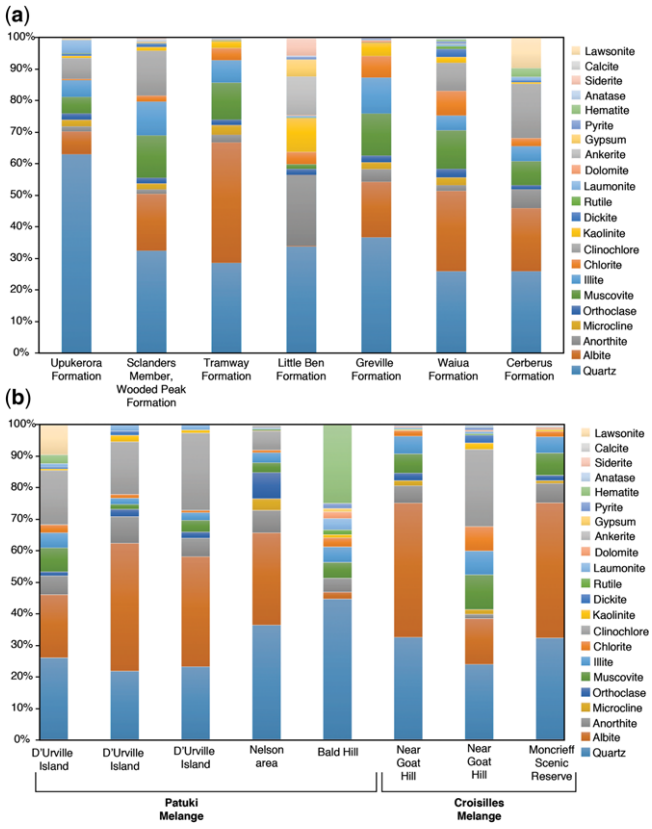

Fig. 11.5. Semi-quantitative XRD results for selected mudrocks: (**a**) Maitai Group; and (**b**) Patuki Melange. See the Supplementary material for the data and the text for explanation.

and, thirdly, dark-grey mudrocks interbedded with sandstones (one sample from D'Urville Island: Fig. 11.4a; and one from the Nelson area: Fig. 11.4c).

The red iron-rich mudrock depositionally overlying basalt on D'Urville Island (Swamp Bay) is moderately rich in hematite (3%), clinochlore (17%), chlorite llb and illite (5%). Lawsonite is abundant (10%). The red iron-rich sediment from the base of the intact succession at Bald Hill is relatively rich in hematite (25%), and also in quartz (44%), muscovite (5%) and illite (5%). There is also some chlorite llb and minor rutile (1.5%) but feldspar is minimal (2.2% albite). Laumontite is quite abundant (3.6%). The samples of more typical dark-coloured mudrock from D'Urville Island and the Dun Mountain area are quartz-rich (36–45%). Albite is very abundant in both samples (29–35%). Calcic plagioclase is present at moderate levels (6–7%). Microcline (<4%) and orthoclase (<8%) are significant components of one sample. Muscovite occurs at levels of 3–4% and illite at *c.* 3%. The sample from D'Urville Island, which is spatially associated with basalt, is very rich in clinochlore (24%), whereas the sample from the Dun Mountain area contains only 6% of this mineral. Rutile occurs in trace amounts in one of the samples. Laumonite is present (2%) in one sample. Calcite, dolomite and siderite are effectively absent. Trace amounts of pyrite occur in one sample.

For comparison, three samples of dark mudrock were analysed from the Croisilles Melange (Fig. 11.1), an additional melange unit (Dickins *et al.* 1986; Landis & Blake 1987; Begg & Johnston 2000), which is intercalated with the Caples Terrane further east (Bishop *et al.* 1976; Turnbull 2000; Mortimer *et al.* 2014). The Croisilles Melange is interpreted by Robertson (2019*a*) as part of the Patuki Melange, as originally formed, that was re-thrust westwards and entrained within the Caples Terrane after Triassic time. Two of the samples are spatially associated with basaltic rocks. Both of these are rich in clininoclore (16–25%) and chlorite 11b (up to 8%). Two samples are also very rich in albite (36–38%), with small amounts of more calcic plagioclase (<6%). Muscovite is abundant (up to 11%) and also illite (up to 8%). Traces of laumontite are present. One sample contains 5% kaolinite and dickite, combined. Carbonate minerals (calcite, dolomite, siderite) are minimal.

Chemical results

In the following subsections, the data that are listed in Supplementary material Tables S3–S6 are used to address specific issues related to the alteration and provenance of the mudrocks.

Major element associations. Selected cross-plots of the data are shown in Figure 11.6 (see the Supplementary material for additional cross-plots of both the Maitai Group and the Patuki Melange).

For the Maitai Group, TiO_2 v. SiO_2 (Fig. 11.6a) and Fe_2O_3 v. SiO_2 (Fig. 11.6b) exhibit generally negative correlations. TiO_2 and Fe_2O_3 tend to increase upwards in the succession, whereas SiO_2 decreases. TiO_2 v. MgO (Fig. 11.6c) and TiO_2 v. Al_2O_3 (Fig. 11.6d) have generally positive correlations, with overall increasing absolute abundances upwards. In addition, Fe_2O_3 and MgO exhibit positive relationships with Al_2O_3 (Fig. 11.6e, f), again with generally increasing abundance upwards. The main exceptions to the above trends are one sample from the Wooded Peak Formation and one from the Little Ben Formation, which have relatively low SiO_2 but high CaO. The Wooded Peak Formation is a marl from low in the succession (West Dome), whereas the Little Ben Formation sample is likely to have undergone post-depositional alteration.

The Tramway and Little Ben formations are compositionally grouped, except for samples with low SiO_2. In contrast, samples from the Wooded Peak Formation exhibit a large range of major element oxide values, similar to the entire range of the Maitai Group. Samples from the overlying Stephens Subgroup have the largest spread of major element oxide data and the lowest SiO_2 values. Samples from the Greville and Waiua formations are compositionally similar to those of the overlying Stephens Subgroup but with a smaller range in major element oxide values.

The equivalent binary plots for the melange mudrocks are more scattered (Fig. 11.6g–l). TiO_2 and Al_2O_3 values range between 0.5–1.7 wt% and 15–23 wt%, respectively. TiO_2, Fe_2O_3, CaO and MnO show negative correlations with SiO_2. The interlava and supra-lava reddish shale from D'Urville Island (Swamp Bay: Fig. 11.4a), shale from above the alkaline basalt in the same area, red siliceous mudrock from Taipare Bay (Fig. 11.4b), Bald Hill (Fig. 11.4d), and also dark shale from the sequence above basalt within the Coal Hill Inclusion (Fig. 11.4e) are all generally grouped, with moderate ranges of SiO_2 (53–64 wt%), TiO_2 (0.5–1.0 wt%), Fe_2O_3 (6–12 wt%) and Al_2O_3 (14–18 wt%). One sample of interlava siliceous mudrock (chert) has a high SiO_2 content (77 wt%) and is correspondingly depleted in other major element oxides, except for CaO (*c.* 6 wt%), which may be enriched by hydrothermal alteration. Dark-grey indurated mudrocks from blocks and small thrust slices within the Patuki Melange range in SiO_2 from relatively low values (*c.* 40 wt%) to relatively high values (*c.* 70 wt %). The samples of red shale from above the alkaline pillow lava from D'Urville Island (Swamp Bay), and also a sample of pakohe from the Dun Mountain area (near Maori Quarry: Fig. 11.4c), are both unusually rich in TiO_2 (>1%).

Major element comparisons

The mudrocks are compared with Post-Archean Australian Shale (PAAS) (Taylor & McLennan 1985) in Figure 11.7, although the more widely used North Atlantic Shale Composite (NASC) (Gromet *et al.* 1984) gives very similar results. For the lower Maitai Group formations (Fig. 11.7a), the main difference from PAAS is that CaO is enriched in one sample of marl from the lower part of the Wooded Peak Formation (West Dome), which is related to large amounts of biogenic carbonate (bivalve detritus). Also, Na_2O is generally enriched reflecting the presence of albite, as indicated by XRD. The samples from the higher Maitai Group formations are mostly tightly grouped, nearer to PAAS than for the lower formations (Fig. 11.7b). The two samples from the Little Ben Formation are unusually calcareous and also enriched in P_2O_5. As there is very little evidence of biogenic material in the Little Ben Formation, it is likely that the high carbonate and phosphate contents relate to post-depositional alteration.

The normalized plots for the melange (Fig. 11.7c) are broadly similar to PAAS, with the exception of CaO, which is strongly depleted in one sample overlying the alkaline basalt on D'Urville Island (Fig. 11.4a); this is likely to represent a hydrothermal alteration effect. Three samples are relatively depleted in K_2O (from Dun Mountain, Taipare Bay and D'Urville Island), which is probably again the result of post-depositional alteration. Several red mudstones containing hematite (from D'Urville Island and Bare Hill) are relatively enriched in MnO.

Alteration state inferred from major element indices

Any interpretation of the mudrocks depends on an understanding of how the mineral content and chemical composition could

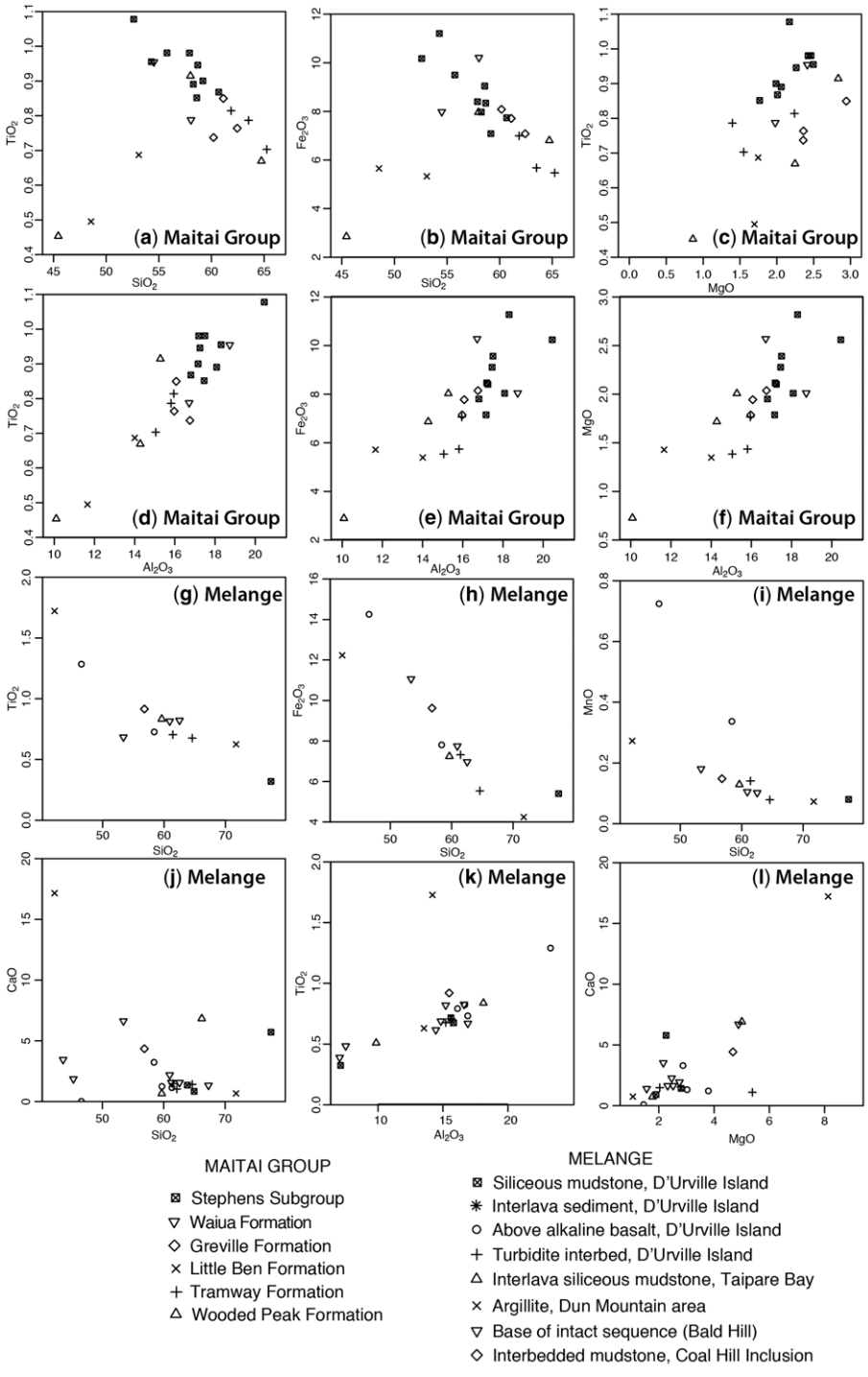

Fig. 11.6. Selected major element variation plots for mudrocks of the Maitai Group (a–f) and the structurally underlying Patuki Melange (j–l). See the text for an explanation. (**a**) TiO_2 v. SiO_2; (**b**) Fe_2O_3 v. SiO_2; (**c**) TiO_2 v. MgO; (**d**) TiO_2 v. Al_2O_3; (**e**) Fe_2O_3 v. Al_2O_3; (**f**) MgO v. Al_2O_3; (**g**) TiO_2 v. SiO_2; (**h**) Fe_2O_3 v. SiO_2; (**i**) MnO v. SiO_2; (**j**) CaO v. SiO_2; (**k**) TiO_2 v. Al_2O_3; and (**l**) CaO v. MgO.

have changed after deposition. The A–CN–K (Al_2O_3 v. CaO + Na_2O v. K_2O) chemical index plot (Bock *et al.* 1994; Fedo *et al.* 1995) illustrates the relative degree of alteration and also the trends in alteration. The Maitai Group samples (Fig. 11.8a) generally plot along the predicted weathering trend, with the majority at the relatively weathered 'clay-rich' end of the spectrum. Many samples plot near the PAAS. Several samples from the Tramway and Little Ben formations plot near the less-weathered end of the trend. The melange data are more scattered (Fig. 11.8b). The most altered samples include the reddish, hematite-bearing shale overlying alkaline basalt on D'Urville Island (Fig. 11.4a), the interlava siliceous mudrock from Taipare Bay (Fig. 11.4b) and the reddish hematite-rich mudstone from the base of the intact sequence at Bald Hill (Fig. 11.4d). Surprisingly, given their highly deformed state, the melange mudrocks are notably less altered than those of the Maitai Group.

The CIA v. ICV plot is a graphical comparison of the chemical index of alteration (CIA) (Nesbitt & Young 1982) and the index of chemical variation (ICV) (Cox *et al.* 1995), as defined by Potter *et al.* (2005) using data from Lee (2002). The Maitai Group data mostly group near the basalt alteration trend (Fig. 11.8c). Two samples from the Little Ben Formation plot closer to 'fresh basalt', which is consistent with the abundance of relatively unaltered basaltic debris, and with the feldspar composition determined by XRD (see above). The melange data are more scattered (Fig. 11.8d) but mostly lie near the basalt alteration trend.

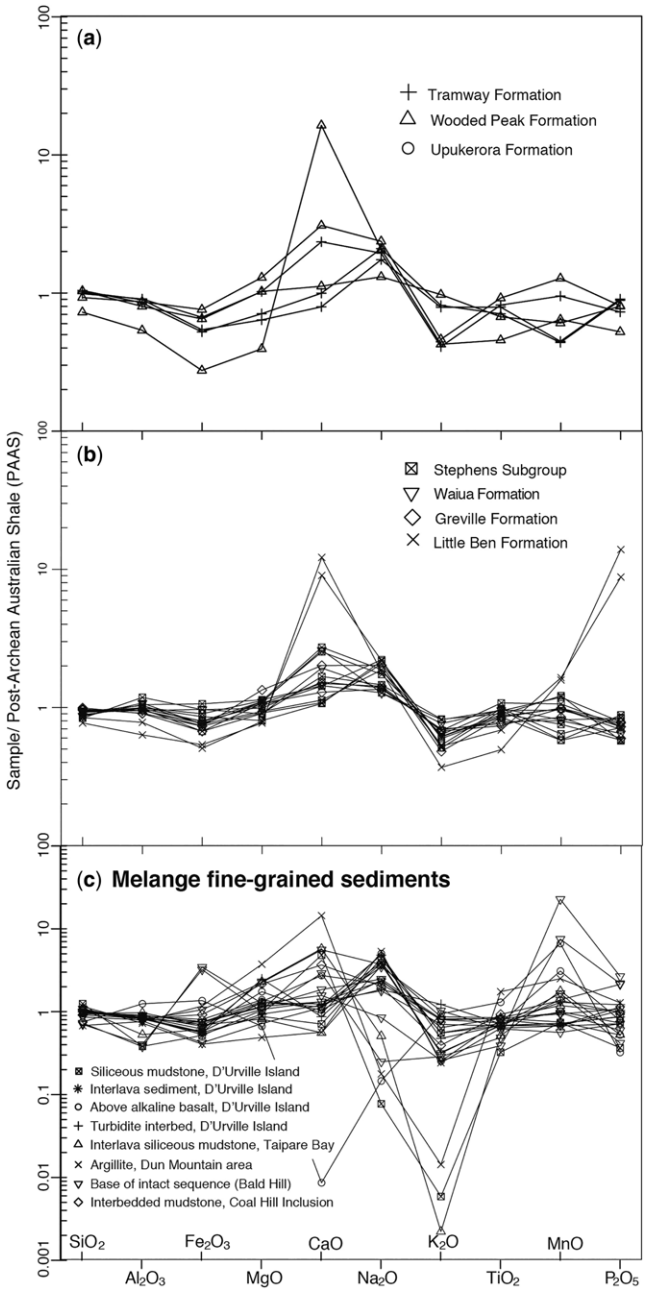

Fig. 11.7. Spider plots of mudrocks from: (**a**) & (**b**) the lower and upper Maitai Group formations and (**c**) the melange units normalized against the composition of PAAS (Taylor & McLennan 1985). PAAS is similar to NASC (Gromet *et al.* 1984). Note: The Permian–Triassic boundary is likely to be located near the base of the Little Ben Formation (Krull *et al.* 2000).

Source discrimination plots

Several well-known source discrimination plots (Bhatia 1983; Bhatia & Crook 1986) help to indicate the provenance of the mudrocks. Such diagrams must be treated with caution, especially because they are based on the study (using a limited number of samples) of one particular area, the New England Orogen which did not include all possible tectonic settings (Armstrong-Altrin & Verma 2005). Also, the diagrams were mainly developed for sandstones. However, the diagrams are useful to indicate trends in the chemical data and are not used here by themselves to assign unique tectonic settings of deposition.

On the La/Th v. Hf diagram (Bhatia & Taylor 1981; McLennan *et al.* 1993), most of the samples plot in the felsic island-arc field, with some from the Maitai Group higher formations tending towards mixed felsic and mafic sources (Fig. 11.9a). On the Th/Sc v. Zr/Sc plot (Bhatia & Crook 1986), the samples all lie on a relatively evolved mantle trend, with none indicative of sediment recycling (mantle addition) (Fig. 11.9b). On the Th/U v. Th plot (McLennan *et al.* 1993), most of the mudrocks are consistent with a continental origin, although two samples from the upper formations of the Maitai Group plot within the depleted mantle source field (Fig. 11.9c).

The provenance of the mudrocks could, in principle, include the Early Permian oceanic arc rocks of the Brook Street Terrane, as exposed in the Takitimu Mountains, south of the Alpine Fault, the late Early Permian supra-subduction zone Dun Mountain ophiolite, the Permian–Triassic arc rocks of the Median Batholith and/or Paleozoic–early Mesozoic metasedimentary rocks of the Western Province (see Robertson *et al.* 2019*a*) (Fig. 11.1). Fields of these potential source units are indicated in Figure 11.9d, e. On the La/Th v. Hf diagram (Fig. 11.9d), the samples mostly plot outside the field of the Brook Street Terrane intrusive and extrusive igneous rocks (see Robertson & Palamakumbura 2019a for the data source) and the Western Province metasedimentary rocks (Campbell *et al.* 1998) but are within the field of the Dun Mountain ophiolite basalts (see Robertson 2019*b* for the data source). On the Ti/Zr v. La/Sc plot (Fig. 11.9e), the samples plot within the intergradational field of primitive to evolved intrusive rocks of the Median Batholith (Muir *et al.* 1998; Price *et al.* 2006, 2011; McCoy-West *et al.* 2014). The samples also plot near the La-rich end of the Western Province Metasediments A field, which represents the dominant compositional range of Late Paleozoic–Early Mesozoic metasedimentary rocks of the Western Province (Campbell *et al.* 1998). The mudrocks from the Patuki Melange plot similarly on the equivalent diagrams, other than one sample of pakohe from the Dun Mountain area (Fig. 11.9f, j).

Taken together, the Median Batholith igneous rocks, the Western Province metasedimentary rocks and the Dun Mountain ophiolite can be all considered as potential source units for both the Maitai Group and the Patuki Melange mudrocks. The relatively non-evolved basaltic rocks of the Brook Street Terrane are effectively ruled out in this regard (e.g. Takitimu Mountains). However, relatively evolved igneous rocks do occur in the Brook Street Terrane arc rocks (Grampian Formation) to the north of the Alpine Fault (Robertson & Palamakumbura 2019*a*) and could represent a suitable mudrock source.

Rare earth element fractionation

The mudrocks from both the lower and upper formations of the Maitai Group are systematically enriched in light REEs (LREEs) relative to heavy REEs (HREEs). A small negative Eu anomaly in most samples reflects plagioclase fractionation (Rollinson 1993) (Fig. 11.10a, b). The REE patterns overlap with the compositional range of basalts from the northern Cascades continental margin arc, western USA, which is shown for comparison (Mullins & Weis 2015) but are dissimilar to basalts of the typical oceanic Izu–Bonin arc (Taylor & Nesbitt 1998).

The normalized REE trends (Gromet *et al.* 1984) for the Maitai Group lower formations are slightly depleted relative to NASC, whereas the HREEs are similar to only slightly depleted (Fig. 11.10c). There is a slight positive Eu anomaly in all but one of the samples, reflecting the feldspar content. The sample from the Little Ben Formation has a flat REE pattern and is slightly enriched relative to NASC. The Maitai Group higher formations have slightly depleted LREEs and similar, to slightly-enriched, HREEs, again with positive Eu anomalies (Fig. 11.10d).

The Maitai Group REE patterns are broadly similar to average upper continental crust (UCC), especially HREEs

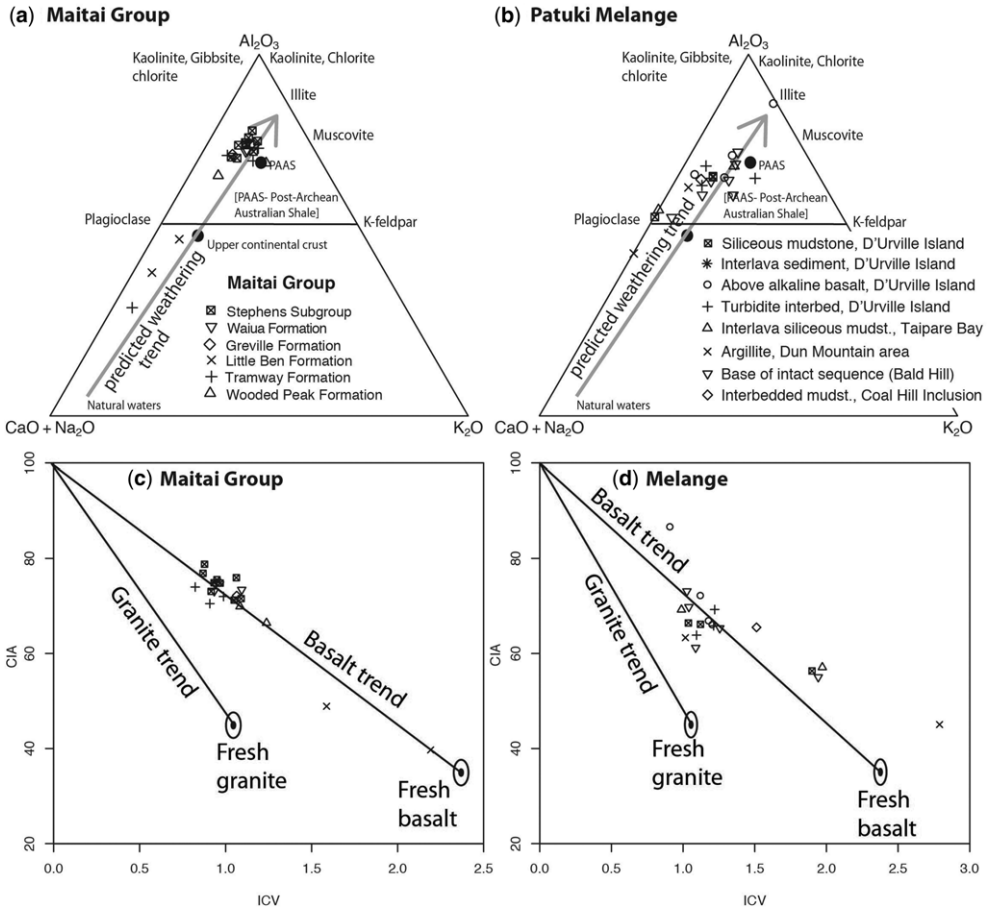

Fig. 11.8. Assessment of chemical alteration: (**a**) & (**b**) A–CN–K (Al_2O_3 v. $CaO + Na_2O$ v. K_2O) plot for the Maitai Group and the Patuki Melange, respectively; and (**c**) & (**d**) CIA v. ICV plot) for the Maitai Group and the melange unit, respectively. See the text for discussion.

(Fig. 11.10e, f). Hf is notably depleted, especially in the Maitai Group higher formations. All of the samples show marked negative Nb anomalies. Several of the lighter REE elements behave erratically (Cs, Rb, Ba, Sr), probably owing to alteration.

Chondrite-normalized REE patterns for the melange mudrocks are broadly similar to those of the Maitai Group (Fig. 11.10g). One of the samples of red hematite-bearing mudrock that depositionally overlies alkaline basalt on D'Urville Island (Fig. 11.4a) is significantly enriched in REEs, except for the lightest REEs (La, Ce and Pr). NASC-normalized REEs (Fig. 11.10h) of the melange mudrocks are similar to those of the Maitai Group as a whole, with the exception of the mudrock above the alkaline basalt, which is highly enriched in HREE (although slightly enriched to depleted in the lightest LREEs). Red mudrock from D'Urville Island (associated with alkali basalt) is generally similar to enriched mid-ocean ridge basalt (E-MORB), in contrast to the other mudrocks (Fig. 11.10i). The melange mudrocks are generally similar to UCC, except for the same sample from D'Urville Island. LREEs (e.g. Sm, Rb, Ba, Th) are strongly depleted in several samples, probably reflecting differential alteration (Fig. 11.10j).

The mudrocks were also compared with intrusive igneous rocks of the Median Batholith and the adjacent country rocks of the Western Province, utilizing chondrite-normalized data from the GNS Science Petlab database (see Robertson & Palamakumbura 2019*c*). The Maitai Group mudrocks overlap with the relatively evolved Triassic-aged Median Batholith intrusive rocks, which have similar HREE, LREE and Eu anomaly patterns (Fig. 11.11a). One sample from the Little Ben Formation is slightly enriched compared to the Median Batholith data. The Maitai Group data are also comparable with limited available REE data for the Permian–Triassic metasedimentary rocks of the Western Province (Robertson & Palamakumbura 2019*c*) (Fig. 11.11b), which formed part of the Gondwana continental margin prior to Late Cretaceous rifting of the Tasman Sea Basin (Mortimer *et al.* 1999).

The normalized mudrock data from the melange are similar to those of the Median Batholith (Fig. 11.11c), except for one sample of iron-rich mudstone from the base of the intact sequence at Bald Hill (Fig. 11.4d). The normalized data are also similar to the Western Province metasedimentary rocks, other than for the same sample from Bald Hill (Fig. 11.10d). When the Permian Formations and the melange matrix are plotted together, a close similarity is apparent, other than for the one sample of hematitic mudstone from Bald Hill (Fig. 11.11e).

Comparison with potential igneous source rocks

The degree of magmatic enrichment or depletion of an igneous source rock is known to be indicated by its chondrite-normalized ratio of La and Yb (La_{CN}/Yb_{CN}) (see the Supplementary material for the method). La_{CN}/Yb_{CN} ratios were calculated for the Maitai Group and the Patuki Melange mudstones using average chondrite values (Boynton 1984). The Maitai Group ratios range from 2.3 to 6.8, whereas those for the melange range from 1.1 to 7.8 (mostly 4.8–7.8). The overall enrichment in LREEs relative to HREEs is characteristic of an undissected arc, to a dissected continental arc (Long *et al.* 2008). Within the Maitai Group, La_{CN}/Yb_{CN} varies throughout the succession as a whole, with the highest values in the Upukerora Formation (4.3), the Wooded Peak Formation (4.7–5.7) and the Tramway Formation (5.6–6.2). La_{CN}/Yb_{CN} in the Little Ben (2.5–6.8) and Greville (3.0–6.0) formations indicates an intermediate-igneous composition. La_{CN}/Yb_{CN} for the Waiua Formation (3.4–4.8) and Stephens Subgroup (2.3–5.4) are generally the lowest in the Maitai Group.

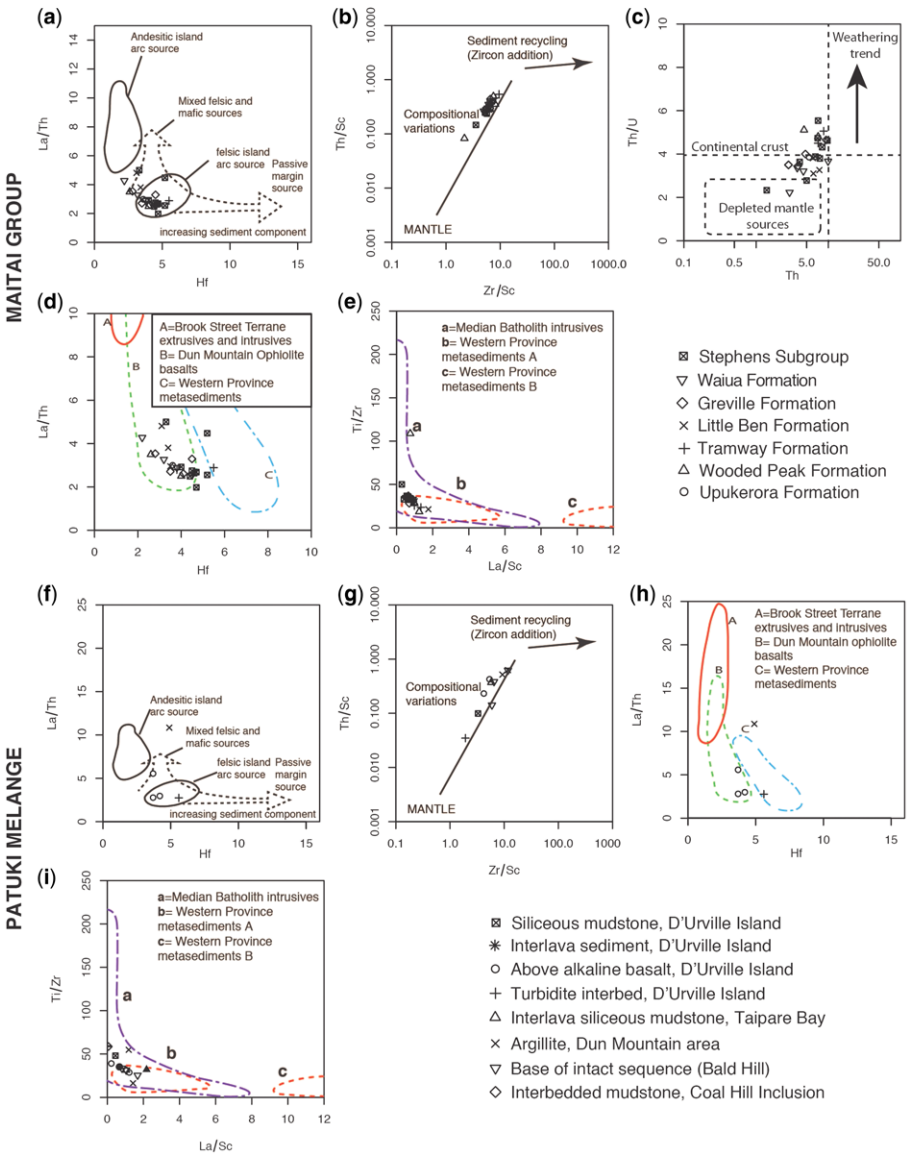

Fig. 11.9. Geochemical discrimination plots of mudrocks. Maitai Group (a–e) and Patuki Melange (f–i): (**a**) La/Th v. Hf; (**b**) Th/Sc v. Zr/Sc; (**c**) Th/U v. Th; (**d**) La/Th v. Hf; (**e**) Ti/Zr v. La/Sc; (**f**) La/Th v. Hf; (**g**) Th/Sc v. Zr/Sc; (**h**) La/Th v. Hf; (**i**) Ti/Zr v. La/Sc.

Geochemistry of ferruginous mudrocks

Mudrocks (and some associated sandstones) are commonly reddish coloured in the Triassic Waiua and Cerberus formations (Stephens Subgroup) (Fig. 11.3f, h). Reddish fine-grained sedimentary rocks also occur within, and depositionally overlie, the alkaline basalts in the Patuki Melange on D'Urville Island, as noted above (Fig. 11.4a). Reddish to greenish mudstones are interbedded with siltstone and fine-sandstone turbidites elsewhere in the same area (Swamp Bay). Red mudstone also occurs at the base of the locally intact sequence within the Patuki Melange at Bald Hill (Fig. 11.4d). Several analyses of hydrothermally enriched metalliferous sediments were previously reported from within the OIB-type basaltic sequence on D'Urville Island and elsewhere (Sivell 2002). The objective here was to determine if the source of the metal content was also hydrothermal or instead detrital or authigenic (i.e. indigenous precipitate).

On the Al v. Fe v. Mn plot (Fig. 11.12a, b), all of the samples from both the Maitai Group and the Patuki Melange plot very close to the Al–Fe baseline, well away from the field of pelagic sediments or hydrothermal deposits. On the Fe v. Mn v. (Ni + Cu + Mn) × 10 plot (Fig. 11.12c, d), which is useful in distinguishing terrigenous, hydrogenous and hydrothermal origins (Bostrom *et al.* 1969; Bonatti *et al.* 1972), the reddish mudrocks from the Maitai Group plot near the Fe apex but with significant amounts of Ni + Cu + Co. Both the interlava and supra-lava red mudstones from D'Urville Island (Swamp Bay) plot at the Fe apex. These results are similar to the composition of halmyrolytic mudstone (i.e. affected by cold seawater interaction) but differ from the composition of a black hydrothermal crust on basalt from the same area (Sivell 2002).

Discussion

Interpretation of mineral content

In general, the minerals present in the Maitai Group represent the combined influences of primary provenance, diagenesis, metamorphism and alteration. All of the samples are relatively carbonate-poor, which could reflect seafloor dissolution (in cold seawater) rather than an absence of supply. This is consistent with the common presence of carbonate fossil moulds, especially in the Tramway Formation.

The quartz-rich sample from the basal Upukerora Formation is likely to contain abundant reworked felsic tuffaceous material. Some terrigenous material is also present (muscovite, illite, rutile), which indicates that deposition took place adjacent to a continental margin. Illite may form diagenetically (Chamley 1989) but its abundance in the samples studied generally correlates with terrigenous content, as supported by the

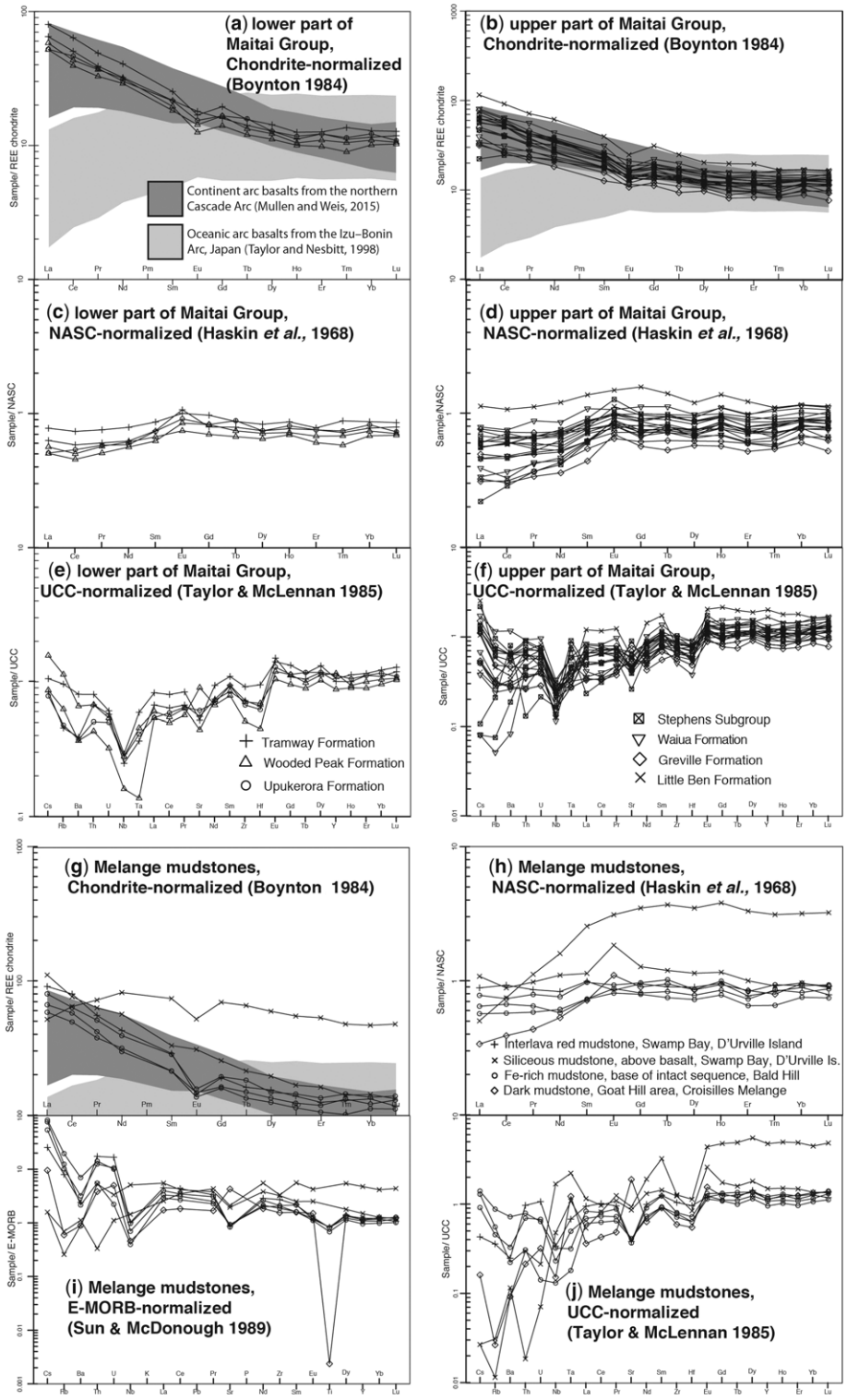

Fig. 11.10. REEs of mudrocks from the lower and upper Maitai Group formations and the Patuki Melange, normalized against different potential source compositions. (**a**) REEs of Maitai Group lower formations v. chrondrite; (**b**) REEs of Maitai Group upper formations v. chrondrite; (**c**) Maitai Group lower formations v. NASC; (**d**) Maitai Group upper formations v. NASC; (**e**) Maitai Group lower formations v. UCC; (**f**) Maitai Group upper formations v. UCC; (**g**) melange REEs v. chondrite; (**h**) melange REEs v. NASC; (**i**) melange REEs v. E-MORB; and (**j**) melange REEs v. UCC. Note: REE-normalizing values from Boynton (1984).

co-occurrence of muscovite. There is also abundant mafic or intermediate-composition igneous material, altered to clinochlore. Feldspars are largely albitized. The laumontite is likely to have formed after maximum burial, by comparison with the Murihiku Terrane elsewhere in South Island (Boles & Coombs 1975; Boles 1991). The sample from the lower part of the Wooded Peak Formation (Sclanders Member) records a high input of terrigenous material (quartz, muscovite, illite), together with alteration to clinochlore of mainly basic igneous material, and albitization of feldspars. The Tramway Formation sample is similarly rich in terrigenous material (quartz, muscovite, illite), albitized feldspar and contains chlorite llb (4%) (rather than clinochlore). Chlinoclore is inferred to change to chlorite llb at *c.* 200°C, although this transformation can be affected by other factors including grain size (e.g. Walker 1991). The Little Ben Formation is strongly feldspathic, mostly in the form of little-altered Ca-rich plagioclase (recorded as anorthite), rather than albite. Terrigenous input is present but muted. The most likely source of the very high quartz is reworked felsic tuff. The origin of the baryte, gypsum and siderite (together making up 23% of the sample) could relate to fluid flow during late-stage mineralization. The Greville and Waiua formations mark a return to a strongly terrigenous input, rich in quartz, muscovite and illite, together with abundant albitized feldspar and altered mafic igneous material, as represented by high clinochlore or chlorite llb. The Cerberus

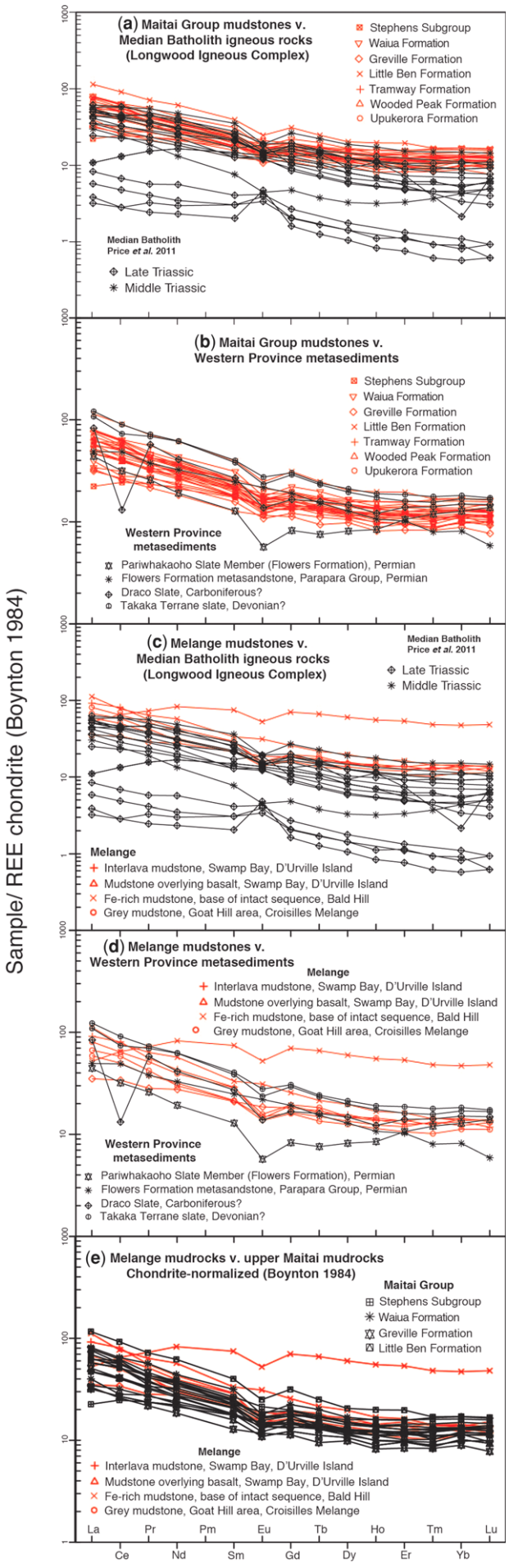

Formation is again terrigenous-rich. However, it also contains a relatively high abundance of relatively unaltered plagioclase, which reflects a high volcanic input (similar to the Little Ben Formation), in agreement with the geochemistry. Consistent with its oxidized red colour, hematite is present (but not pyrite) in the Cerberus Formation. Laumontite is present in minor amounts high in the succession, probably again related to burial metamorphism. Minor kaolinite is likely to have formed during diagenesis (although a primary input cannot be excluded), followed by partial transformation to dickite during burial (e.g. Ehrenberg *et al.* 1993; Beaufort *et al.* 1998). Notably, lawsonite is highly abundant (10%) in the Cerberus Formation (see below).

The typical mudrocks of the Patuki Melange (and the Croisilles Melange) are terrigenous, with relatively abundant quartz, muscovite and illite. These sediments are also strongly feldspathic, probably reflecting an input mainly from intermediate-composition volcanic rocks, as supported by the geochemistry and the petrography of interbedded sandstones (Robertson & Palamakumbura 2019*b*). Feldspars were largely albitized during burial. The clinochlore-rich sample from D'Urville Island is likely to represent alteration of material derived from the underlying basalt. Minor laumontite probably developed as in the Maitai Group. The reddish-coloured, hematite-bearing mudrock from the same area, depositionally overlying basalt, is compositionally similar to the typical mudrocks but has iron-oxide enrichment (Fig. 11.12), reflecting an oxidizing depositional setting. Laumontite is again present. The sample of red mudrock from Bald Hill (Fig. 11.4d) is again terrigenous, with very abundant quartz and also illite but minimal plagioclase. The source could be felsic volcanism (or even aeolian). The reddish well-oxidized sediments (D'Urville Island and Bald Hill) are likely to represent slow accumulation, prior to the arrival of sandstone turbidites, which dominate the overlying successions in both areas (Robertson 2019*a*). The lawsonite, which was locally detected in both the Maitai Group (Cerberus Formation) and the Patuki Melange (D'Urville Island), is indicative of very deep burial metamorphism (>15 km). The origin of the lawsonite in these rocks is poorly understood, especially as it occurs spasmodically. The very deep burial was possibly tectonically imposed during the Early Cretaceous Rangitata Orogeny (Landis 1974; see Robertson *et al.* 2019*b*).

The three samples of mudrock from the Croisilles Melange are again terrigenous, with the addition of common clinochlore (up to 25%) and chlorite 11b (up to 8%), which are likely to have been derived from associated basaltic rocks. The chlorite-rich sediment was initially derived locally from basaltic rocks, followed by emplacement into the melange (see Robertson 2019*a*).

Interpretation of major element trends

The decrease in SiO_2 v. increase in TiO_2, Fe_2O_3, Al_2O_3 and MgO upwards in the Maitai Group is interpreted to indicate a long-term change in provenance. The relative increases in TiO_2 and Fe_2O_3 are suggestive of increasing input from mafic minerals or basic rock detritus stratigraphically upwards (Gu *et al.* 2002). The decreasing SiO_2 upwards is consistent with a change from a relatively evolved, intermediate-composition igneous source in the lower formations of the Maitai Group

Fig. 11.11. Normalized plots of REE abundances in mudrocks v. comparative units elsewhere in South Island. One sample is included from the Croisilles Melange (see the Supplementary material). (**a**) Maitai Group v. Median Batholith (Longwood Igneous Complex); (**b**) Maitai Group v. Western Province metasedimentary rocks; (**c**) melange v. Median Batholith; (**d**) melange v. Western Province metasedimentary rocks; and (**e**) melange v. upper Maitai Group formations.

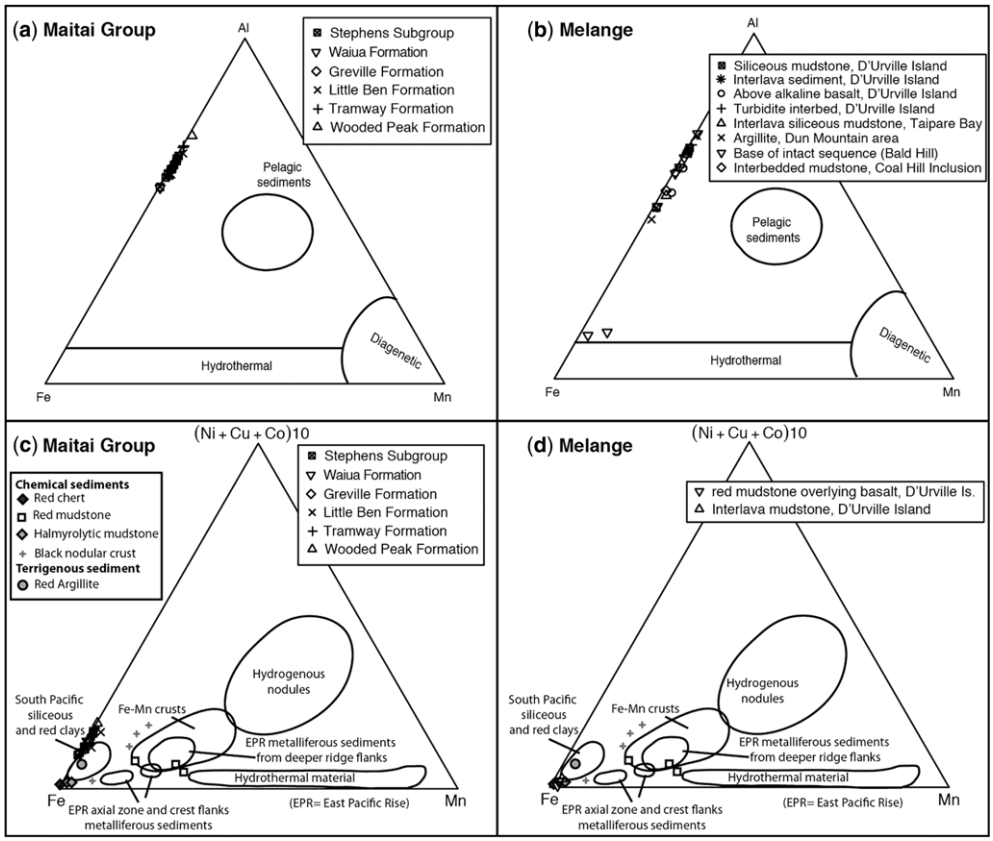

Fig. 11.12. Plots of red iron-rich sediments from the upper Maitai Group (Cerberus Formation) and locally from the Patuki Melange. (**a**) Al v. Fe v. Mn plot for the Maitai Group; (**b**) Al v. Fe v. Mn plot for the Patuki Melange; (**c**) Fe v. Mn v. (Ni + Cu + Co) × 10 for the Maitai Group; (**d**) Fe v. Mn v. (Ni + Cu + Co) × 10 for the Patuki Melange. Also shown are samples analysed by Sivell (2002) associated with basaltic rocks and terrigenous sediments in the type area of the Patuki Melange on D'Urville Island (Swamp Bay). Several deep-sea sediment compositions are shown for comparison (e.g. Bostrom *et al.* 1969; Bonatti *et al.* 1972; Sayles & Bischoff 1973; Cronan 1976). See the text for explanation.

(Wooded Peak and Tramway formations), to a less-evolved, more basic source in the higher formations (Little Ben Formation and upwards). An alternative explanation of the marked increases in Al_2O_3 and Fe_2O_3 concentrations up-sequence is that they reflect increases in clay minerals such as illite and kaolinite (Lee 2002; Yan *et al.* 2012), although this is not supported by the available XRD data. The change from slightly depleted patterns relative to PAAS in the lower Maitai Group formations (Fig. 11.7) to a more PAAS-like composition in the higher formations is suggestive of an overall change from a relatively evolved, felsic source to a more mafic, grandioritic-type source (Taylor & McLennan 1985; Yan *et al.* 2012). A similar pattern is seen in the associated sandstones, although the degree of fractionation varies regionally and temporally (Robertson & Palamakumbura 2019*b*).

A similar interpretation applies to the melange mudrocks. The siliceous interlava (chert) sample (SiO_2 77.40 wt%) from Taipare Bay (Fig. 11.4b) has similarities with the high-silica argillite (SiO_2 71.73 wt%) from the Dun Mountain area, with correspondingly low concentrations of TiO_2, Fe_2O_3 and Al_2O_3, and a high Al_2O_3/TiO_2 ratio (*c.* 22) (see the Supplementary material), which are suggestive of an andesitic to felsic source (McLennan *et al.* 1993). The low-silica sample from near the base of the intact succession at Bald Hill (Fig. 11.4d) has a Al_2O_3/TiO_2 value of *c.* 8, which is suggestive of a mafic source (Le Maitre 1976; Girty *et al.* 1996). In contrast, the high-silica sample from Taipare Bay has a Al_2O_3/TiO_2 value of *c.* 21, which is suggestive of an andesitic to rhyodacitic source. Samples with relatively low Al_2O_3 and which are similar to PAAS, including two from near the base of the intact sequence at Bald Hill (7.52 and 7.05 wt%), according to Hayashi *et al.* (1997) correspond to a low feldspar (6.6% total) but high clay mineral content (8.7%), which is in agreement with the XRD data. In addition, the low-silica pakohe sample (42.17 wt%) from near Maori Quarry in the Dun Mountain area (Fig. 11.4c) has high TiO_2 and Fe_2O_3 contents and is slightly enriched relative to PAAS, which is suggestive of high concentrations of mafic minerals or mafic rock fragments. The pakohe is generally found enclosed within, or spatially associated with, intrusive ophiolitic rocks and is inferred to represent fine-grained terrigenous sediment that accreted to the base of the supra-subduction zone Dun Mountain ophiolite in a forearc setting (Robertson 2019*a*).

The two shale samples from above alkali basalt on D'Urville Island (Swamp Bay: Fig. 11.4a) are enriched in MnO compared to the other samples and PAAS. One of these samples is also enriched in TiO_2, Al_2O_3 and Fe_2O_3, and contains hematite and relatively abundant clinochlore. The relatively high TiO_2 and Al_2O_3 are explained by submarine erosion of the underlying alkaline basalts. The remaining melange data are well grouped and have intermediate (i.e. andesitic) compositional signatures but with small variations (e.g. Bald Hill v. Coal Hill). Al_2O_3/TiO_2 range from *c.* 16 to *c.* 22, within the range of undifferentiated UCC and PAAS (Le Maitre 1976; Girty *et al.* 1996). Slight enrichments in Na_2O and depletions of K_2O reflect differential alteration and metamorphism, as for the Maitai Group. Alteration indices vary considerably between the melange samples (mostly 54–69), below the average CIA range of 70–75 for shale (Nesbitt & Young 1982). Most of the melange mudrocks were apparently derived from a less-weathered source than those of the Maitai Group. The ICV indices (0.9–2.8) for the melange samples suggest variable weathering and alteration.

Interpretation of alteration indices

The position of the Tramway Formation sample towards the $CaO + Na_2O$ axis on the A–CN–K plot (Fig. 11.8a) is a consequence of the typically high bioclastic content, including bivalve fragments (Robertson & Palamakumbura 2019*b*). The Little Ben Formation also plots towards the $CaO + Na_2O$ axis, although minimal calcium carbonate is present. The likely cause is the abundance of relatively unaltered Ca-plagioclase,

as indicated by XRD. Albite is abundant in indurated dark grey mudrock of the Patuki Melange (e.g. Fig. 11.4e) (and also the Croisilles Melange). Metasomatic formation of albite within originally feldspar-rich fine-grained sediment was a key cause of the hardening to form Maori tool-quality pakohe (Johnston 2011). On the other hand, the absence of trends towards the K_2O axis allows K-metasomatism (Fedo *et al.* 1995) to be discounted.

CIA values of 70–85 represent average shale and clay minerals (e.g. muscovite and illite) (Nesbitt & Young 1982). Similar CIA values to those of the Maitai Group and the Patuki Melange (Fig. 11.8c, d) in other examples relate to moderately to strongly weathered source regions, as reported from several ancient settings: for example, the Dahomey Embayment in SW Nigeria (Ejeh 2016), the Vindhyan Supergroup in central India (Paikaray *et al.* 2008) and the Pyeongan Supergroup in Korea (Lee 2002).

ICV values (Fig. 11.8c, d) reflect variations of alumina compared to other cations (Cox *et al.* 1995) and, therefore, illustrate variations between mafic minerals and clay minerals, and also the overall compositional maturity (the lowest ICV values are the most compositionally mature and vice versa) (Lee 2002). ICV values in the Maitai Group range from 0.87 to 2.75, corresponding to the abundance of minerals such as muscovite, illite and chlorite (Cox *et al.* 1995), as confirmed by XRD.

The combined CIA and ICV values show that the Patuki Melange mudrocks are generally more altered than those of the Maitai Group. This can be explained by local derivation of relatively unaltered igneous basic material in the Patuki Melange. In agreement, petrographical evidence shows that many of the sandstones in the Patuki Melange (e.g. from the Coal Hill Inclusion: Fig. 11.4, location 3) contain abundant relatively unaltered basic ophiolitic or arc-derived extrusive igneous rock debris (Robertson & Palamakumbura 2019*c*).

Interpretation of trace and REE data

On the discrimination plots (Fig. 11.9a–e), the Maitai Group data are suggestive of a mafic to felsic arc source, similar to the Median Batholith (Price *et al.* 2011). Th/Sc and Zr/Sc ratios suggest a moderately enriched basaltic to andesitic source (Hassan *et al.* 1999; Armstrong-Altrin *et al.* 2013) (Fig. 11.9b). The relatively low but variable Hf values in the Hf–La/Th plot (Fig. 11.9d) are consistent with mixed mafic and intermediate sources, similar to the Carboniferous and Devonian sediments of the Junggar Basin, central China (Yang *et al.* 2012). The Ti/Zr v. La/Sc plot (Fig. 11.9e) and the Ti/Zr and La/Sc ratios (10–50) (see the Supplementary material) point to a continental-arc source (Bhatia & Crook 1986; Gu *et al.* 2002), similar to the Permian Sangre de Cristo Formation, Colorado, USA (Cullers 2000). The relatively high Ti/Zr v. low La/Sc ratios in the Maitai Group upper formations support an overall change towards a relatively mafic source. However, this was compositionally variable, as suggested by the spread from depleted mantle to weathered continental crust on the Th/U–Th plot (Fig. 11.10c), especially for the Stephens Subgroup (McLennan *et al.* 1993). A similar pattern is, for example, recorded in the Early Cretaceous sediments of the Inner Zone of SW Japan (Asiedu *et al.* 2000).

There is a slight tendency for the mudrocks in the upper part of the Wooded Peak Formation (Waitaramea Member at West Dome, Southland) to have relatively high values of Cr (up to 128 ppm), Cu (up to 61 ppm) and Zn (up to 123 pmm). Detrital input from the underlying Dun Mountain ophiolite is reported for the Upukerora Formation (Pillai 1989; Robertson 2019*b*), and also from the base of the overlying Wooded Peak Formation in the Lee River area (the Anslow Member of Owen 1995) and also in the Maitai River (Robertson & Palamakumbura 2019*b*). The sandstones of the Waitaramea Member are very rich in clinopyroxene and basic volcanic material, hence the high Cr content, and are interpreted to have been derived from the upper, extrusive layer of the subjacent Dun Mountain ophiolite (Robertson & Palamakumbura 2019*c*). The uppermost part of the Wooded Peak Formation at West Dome accumulated in a small basin within the palaeotopography of the emplaced Dun Mountain ophiolite (Robertson & Palamakumbura 2019*b*). Metal enrichment related to an ophiolitic source has also been reported from deep-sea mud-rich sediments elsewhere: for example, in the Neogene back-arc Woodlark Basin, SW Pacific (Robertson & Sharp 2002).

Similar REE patterns in mudrocks to those of the Maitai Group and the Patuki Melange (Fig. 11.10a, b & g) have commonly been explained by an UCC source (Condie 1993), with examples including the Devonian Liuling Group in central China (Yan *et al.* 2012), the Late Miocene Kudankulam Formation in southern India (Armstrong-Altrin *et al.* 2004) and the Precambrian of the Hunan area in Wuhan, south China (Gu *et al.* 2002). On the NASC-normalized plots (Fig. 11.10c, d & h), the broadly flat HREE and LREE patterns of the Maitai Group and the melange support a comparison with weathered continental crust (Taylor & McLennan 1985).

Calculated La_{CN}/Yb_{CN} for the Maitai Group and the Patuki Melange (see the Supplementary material) are typical of undissected to dissected continental arcs (Long *et al.* 2008). The overall decrease in La_{CN}/Yb_{CN} upwards in the Maitai Group suggests a change to a less-enriched source. A comparison of La_{CN}/Yb_{CN} in the Maitai Group v. the melange mudstones suggests that the Maitai Group has a slightly less-enriched source than the melange mudrocks overall.

The slight depletion of REEs relative to NASC and the slight positive Eu anomalies in most of the Maitai Group samples (Fig. 11.10c, d) are consistent with derivation from feldspar-rich igneous rocks. NASC is comparable to the composition of riverine sediments, including the Amazon, Congo, Ganges, Garonne and Mekong (Taylor & McLennan 1985). Average shale composition is, broadly, a proxy for particulate matter supplied via rivers and the atmosphere. The slightly depleted signature of both the Maitai Group and the melange sediments, therefore, points to a more basic (basaltic to andesitic) source than average shale. The larger spread and more depleted nature of the Maitai Group upper formations suggests an upwards increase in relatively basic material within the Triassic Stephens Subgroup, which is also supported by the XRD data (Fig. 11.5) and petrographical evidence from associated sandstones (Robertson & Palamakumbura 2019*b*).

Comparison with average continental crust (UCC) suggests a dual source for both the Maitai Group and the melange mudrocks (Fig. 11.10e, f). The LREEs and HREEs are broadly similar to UCC, suggesting this composition as an important source. However, the Nb and Hf depletion, especially in the Maitai Group upper formations, is consistent with a relatively evolved source, as in active continental margin granites. Granitoid rocks contributed detritus to these upper formations in some areas (Owen 1995; Robertson & Palamakumbura 2019*b*). The additional source is, therefore, likely to have been the calc-alkaline magmatic arc represented by the Median Batholith (Price *et al.* 2011) or its probable equivalent along the Gondwana active continental margin (not exposed). The continental hinterland, including the South Australian Craton (Swain *et al.* 2008), could have also provided material of similar composition. A similar dual origin has been inferred for Precambrian shales of the Cuddapah Basin in India (Manikyamba *et al.* 2008). The Nb and Hf depletion relative to UCC is similar to that of the lower formations of the Maitai Group (Wooded Peak and Tramway formations) and the Western Province metasediments, consistent with a relatively non-evolved continental source.

The REE and trace element data from the Patuki Melange (see Fig. 11.9 and the Supplementary material) are more scattered, particularly Th/Sc and Zr/Sc ratios, which is consistent with multiple depleted to moderately enriched sources (Taylor & McLennan 1985). La/Sc ranges from 0.5, typical of oceanic or undifferentiated crust (McLennan *et al.* 1993), to *c.* 0.8 (locally up to *c.* 2), suggesting a granodioritic composition as in continental-arc crust or differentiated crust (Bhatia & Crook 1986; Kasanzu *et al.* 2008; Long *et al.* 2008). In agreement, the lowest La/Sc ratios are in the interlava siliceous mudrock from Taipare Bay (Fig. 11.4b) and the supra-lava silty mudstone from the Coal Hill Inclusion (Fig. 11.4e). The higher ratios are in the dark shales generally and in the red shales from the base of the local intact sequence at Bald Hill (Fig. 11.4d). Taken as a whole, the Ti/Zr ratios are suggestive of a continental-arc source, as in the Maitai Group (Bhatia & Crook 1986). The range in La/Th ratios and the absolute values of Hf again reflect variable sources. The Ti/Zr v. La/Sc ratios of the melange sediments are indicative of source rocks similar to the Western Province metasediments.

Recent work suggests that the Maitai Group accumulated in the distal, outer part of an undissected forearc basin, which generally evolved from underfilled during the Late Permian to filled during the Early–Middle Triassic (Robertson & Palamakumbura 2019*b*). The mineral and chemical data from the Maitai Group mudrocks are generally compatible with a source in western Queensland or eastern Antarctica, as are comparable chemical data for the associated sandstones (Robertson & Palamakumbura 2019*b*; see also the Supplementary material). However, when detrital zircon geochronology is taken into account (Adams *et al.* 2002, 2007), a source in western Queensland (New England Orogen) is likely, with the implication that the Dun Mountain–Maitai Terrane (including the Patuki Melange) was translated several thousand kilometres southwards (in present coordinates) to reach its present position.

Interpretation of iron-rich sediments

The distinctive iron-enriched mudrocks in the Triassic Waiua and Cerberus upper formations of the Maitai Group are all relatively aluminous and contain hematite. This is consistent with a dominantly detrital input from a landmass that experienced strong chemical weathering. In terms of Mn content, the samples are similar or depleted compared to typical oceanic siliceous clays and red clays. The iron is interpreted to have been derived from Gondwana and accumulated slowly under overall oxidizing seafloor conditions. The Cerberus Formation is relatively fine grained and bioturbated, consistent with oxidizing conditions (Robertson & Palamakumbura 2019*b*). However, Mn is minimal. A possible explanation is that the seafloor (or subseafloor) conditions were dysaerobic (i.e. 0.1–1.0 ml of dissolved oxygen per litre of water), such that Mn remained in solution or, if precipitated, was selectively lost during diagenesis. The red oxidized iron-rich sediments of the melange are interpreted to have a similar terrigenous origin to those of the Maitai Group. This contrasts with black Fe–Mn crusts and some red mudstones within the extrusive sequence on D'Urville Island (Swamp Bay) that are interpreted as hydrothermal precipitates (Sivell 2002) (Fig. 11.12). The latter sediments formed in an oceanic setting, in contrast to the red mudstones analysed during this study which accumulated associated with sand turbidites in a trench or forearc setting (Robertson 2019*a*).

The alkaline basalts from Swamp Bay, D'Urville Island are interpreted as an oceanic seamount that accreted in a subduction trench (Robertson 2019*a*). During or after accretion, the lavas formed a local topographical high on which sediments accumulated relatively slowly, favouring enrichment in iron oxide. The red mudstone thereby formed the base of a succession of deep-water sandstone–mudrock turbidites that accumulated in a trench or trench-slope basin (Robertson 2019*a*). The red mudstones at the base of the intact succession at Bald Hill (Fig. 11.4d) could also represent condensed (slow) sedimentation on a topographical high in a subduction trench or forearc setting, although its substratum is unknown.

Relationship to global extinction and climate change

A global change from an icehouse world to a hothouse world took place gradually at the end of Mid-Permian time and was followed by warm climatic conditions during the Early Triassic (Veevers 1990; Golonka & Ford 2000; Galfetti *et al.* 2007). In eastern Australia this led to the disappearance of ice cover, first in coastal areas and then further inland. Hot and arid periods ensued after the Mid-Permian (Retallack 1999; Retallack & Krull 1999; Chumakov & Zharkov 2003). The climatic change favoured increased chemical weathering on land, creating large volumes of iron oxide and clay minerals, which were transported by rivers to the sea. These sediments were finally delivered to the deep-sea forearc basin and the adjacent subduction trench by gravity-flow processes. The fine-grained material within several of the formations (e.g. Cerberus Formation) was reworked by deep-sea currents. Aeolian transport may have contributed to the fine-grained sediment supply, as in modern basins flanking hot arid regions but is not easily recognizable with the available data.

The mudrocks studied accumulated before, during and after the largest extinction event in Earth history, at the Permian–Triassic boundary (Erwin 1993). Major temperature rise occurred during the latest Permian, before the major extinction event (Joachimski *et al.* 2012), and is likely to have abruptly increased weathering, erosion and supply of fine-grained sediment to the ocean. A major cause is likely to have been the release of isotopically light carbon from Siberian Traps volcanism (Renne *et al.* 1995). Warm climatic conditions during the Early Triassic favoured the accumulation of voluminous red mud during times of reduced coarser-grained clastic sediment supply.

Conclusions

- The mudrocks of the Maitai Group and the structurally underlying Patuki Melange were sourced from variably evolved continental margin arc crust and relatively differentiated continental crust.
- The mudrocks of the Mid–Late Permian lower formations of the Maitai Group were mainly derived from a relatively differentiated continental magmatic arc and related country rocks. Supply switched to a generally less-evolved continental margin magmatic arc and related country rocks during the Early–Mid-Triassic.
- For the Maitai Group, the inferred arc source generally evolved from relatively enriched during the deposition of Maitai Group Permian lower formations (Wooded Peak Formation, Tramway Formation) to more depleted during accumulation of the latest Permian–Middle Triassic upper formations (Little Ben Greville and Waiua formations, and Stephens Subgroup).
- Utilizing chemical alteration indices, the overall degree of alteration increases upwards from the base to the top of the Maitai Group, corresponding to an increase in the amount of fine-grained alumina-silicate material (mica and clay minerals).
- Mudrocks from a range of structural settings within the Patuki Melange represent similar mixed continental margin arc and differentiated continental crust sources, similar to

the Maitai Group. The degree of alteration is generally lower than in the Maitai Group probably because of the presence of an additional source of relatively unaltered basic ophiolite-related material.

- Red iron-rich mudrocks in the Triassic Maitai Group upper formations (Waiua and Cerberus formations) and also within the Patuki Melange reflect the input of fine-grained, oxidized particulate matter from land and accumulation under oxidizing seafloor conditions (mainly during a warm period). The red oxidized sediments in the melange represent slow accumulation on topographical highs in a subduction trench or trench-slope setting.
- The Patuki Melange mudrocks were derived from relatively differentiated continental magmatic arc crust, indistinguishable from that supplying the Late Permian Wooded Peak and Tramway formations (Maitai Group lower formations). The chemical data, therefore, support palaeontological and petrographical evidence that these sediments are of Late Permian age.
- The provenance of the mudrocks in both the Maitai Group and the Patuki Melange is chemically fingerprinted as the Median Batholith and associated country rocks of the Western Province or possible (non-exposed) equivalents in the eastern Australia–Antarctica region.

The underpinning fieldwork was carried out by the second author during the austral summers of 2013, 2014 and 2017. Mike Johnston kindly provided advice on fieldwork in the Nelson area, while Nick Mortimer provided similar pointers for outcrops in Southland. Post-doctoral research by the first author over 8 months was supported by the John Dixon Memorial Fund. Preparation of the samples for chemical analysis was assisted by Malgorzata Musur and Alex Cooke. The XRF and XRD analysis was carried out by Nic Odling. The manuscript benefited from comments by John Armstrong-Altrin and an anonymous reviewer.

References

Adams, C.J., Barley, M.E., Maas, R. & Doyle, M.G. 2002. Provenance of Permian–Triassic volcaniclastic sedimentary terranes in New Zealand: evidence from their radiogenic isotope characteristics and detrital mineral age patterns. *New Zealand Journal of Geology and Geophysics*, **45**, 221–242.

Adams, C.J., Campbell, H.J. & Griffin, W.R. 2007. Provenance comparisons of Permian to Jurassic tectonostratigraphic terranes in New Zealand: perspectives from detrital zircon age patterns. *Geological Magazine*, **144**, 701–729.

Ahn, J.H., Peacor, D.R. & Coombs, D.S. 1988. Formation mechanisms of illite, chlorite and mixed-layer illite–chlorite in Triassic volcanogenic sediments from the Southland Syncline, New Zealand. *Contributions to Mineralogy and Petrology*, **99**, 82–89.

Aitchison, J.C. & Landis, C.A. 1990. Sedimentology and tectonic setting of the Late Permian–early Triassic Stephens Subgroup, Southland, New Zealand: an island arc-derived mass flow apron. *Sedimentary Geology*, **68**, 55–74.

Aitchison, J.C., Landis, C.A. & Turnbull, I.M. 1988. Stratigraphy of Stephens Subgroup (Maitai Group) in the Countess Range–Maroroa River area, northwestern Southland, New Zealand. *Journal of the Royal Society of New Zealand*, **18**, 271–284.

Armstrong-Altrin, J.S. 2015. Evaluation of two multidimensional discrimination diagrams from beach and deep-sea sediments from the Gulf of Mexico and their application to Precambrian clastic sedimentary rocks. *International Geology Review*, **57**, 1446–1461.

Armstrong-Altrin, J.S. & Verma, S.P. 2005. Critical evaluation of six tectonic setting discrimination diagrams using geochemical data of Neogene sediments from known tectonic settings. *Sedimentary Geology*, **177**, 115–129.

Armstrong-Altrin, J.S., Lee, Y.I., Verma, S.P. & Ramasamy, S. 2004. Geochemistry of sandstones from the Upper Miocene Kudankulam Formation, Southern India: implications for provenance, weathering, and tectonic setting. *Journal of Sedimentary Research*, **74**, 285–297.

Armstrong-Altrin, J.S., Nagarajan, R. *et al.* 2013. Geochemistry of the Jurassic and Upper Cretaceous shales from the Molango Region, Hidalgo, eastern Mexico: implications for source-area weathering, provenance, and tectonic setting. *Comptes Rendus – Geoscience*, **345**, 185–202.

Asiedu, D.K., Suzuki, S., Nogami, K. & Shibata, T. 2000. Geochemistry of Lower Cretaceous sediments, Inner Zone of Southwest Japan: constraints on provenance and tectonic environment. *Geochemical Journal*, **34**, 155–173.

Beaufort, D., Cassagnabère, A., Petit, S., Lanson, B., Berger, G., Lacharpagne, J.-C. & Johansen, H. 1998. Kaolinite-to-dickite conversion series in sandstone reservoirs. *Clay Minerals*, **33**, 297–316.

Begg, J.G. & Johnston, M.R. 2000. *Geology of the Wellington Area. 1:260 000*. Institute of Geological and Nuclear Sciences Geological Map, **10**. Institute of Geological and Nuclear Sciences Limited, Lower Hutt, New Zealand.

Bhatia, M.R. 1983. Plate tectonics and geochemical composition of sandstones. *Journal of Geology*, **91**, 611–627.

Bhatia, M.R. 1985. Rare earth element geochemistry of Australian Paleozoic graywackes and mudrocks: provenance and tectonic control. *Sedimentary Geology*, **45**, 97–113.

Bhatia, M.R. & Taylor, S.R. 1981. Trace element geochemistry and sedimentary provinces: a study from the Tasman Geosyncline, Australia. *Chemical Geology*, **33**, 115–126.

Bhatia, M.R. & Crook, K.A.W. 1986. Trace element characteristics of graywackes and tectonic setting discrimination of sedimentary basins. *Contributions to Mineralogy and Petrology*, **92**, 181–193.

Bishop, D.G., Bradshaw, J.D., Landis, C.A. & Turnbull, I. 1976. Lithostratigraphy and structure of the Caples terrane of the Humboldt Mountains, New Zealand. *New Zealand Journal of Geology and Geophysics*, **19**, 827–848.

Bock, B., McLennan, S.M. & Hanson, G.N. 1994. Rare earth redistribution and its effects on the neodymium isotope system in the Austin Glen Member of the Normanskill Formation, New York, USA. *Geochimica et Cosmochimica Acta*, **58**, 5245–5253.

Boles, J.R. 1991. Diagenesis during folding and uplift of the Southland Syncline, New Zealand. *New Zealand Journal of Geology and Geophysics*, **34**, 253–259.

Boles, J.R. & Coombs, D.S. 1975. Mineral reactions in zeolitic Triassic tuff, Hokonui Hills, New Zealand. *Geological Society of America Bulletin*, **86**, 63–173.

Bonatti, E., Kraemer, T. & Rydell, H. 1972. Classification and genesis of submarine iron-manganese deposits. *In*: Horn, D. (ed.) *Ferromanganese Deposits on the Ocean Floor*. National Science Foundation, Washington, 149–165.

Bostrom, K., Peterson, M.N.A., Joensuu, O. & Fisher, D.E. 1969. Aluminium-poor ferromanganese sediments on active ocean ridges. *Journal of Geophysical Research*, **74**, 3261–3270.

Bouma, A.H. 1962. *Sedimentology of Some Flysch Deposits: A Graphic Approach to Facies Interpretation*. Elsevier, Amsterdam.

Boynton, W.V. 1984. Chapter 3. Cosmochemistry of the rare earth elements: Meteorite studies. *In*: Henderson, P. (ed.) *Earth Element Geochemistry*. Developments in Geochemistry, **2**. Elsevier, Amsterdam, 63–114.

Campbell, H.J. 2000. The marine Permian of New Zealand. *In*: Yin, H., Dickins, J.M., Shi, G.R. & Tong, J. (eds) *Permian–Triassic Evolution of Tethys and the Western Circum-Pacific*. Developments in Palaeontology and Stratigraphy, **18**. Elsevier, Amsterdam, 111–125.

Campbell, H.J. 2019. Biostratigraphic age review of New Zealand's Permian–Triassic central terranes. *In*: Robertson, A.H.F. (ed.) *Paleozoic–Mesozoic Geology of South Island, New Zealand: Subduction-related Processes Adjacent to SE Gondwana*. Geological Society, London, Memoirs, **49**, 31–41, https://doi.org/10.1144/M49.6

Campbell, H.J., Smale, D., Grapes, R., Hoke, L, Gibson, G.M. & Landis, C.A. 1998. Parapara Group: Permian–Triassic rocks in

the Western Province, New Zealand. *New Zealand Journal of Geology and Geophysics*, **41**, 281–296.

Cavalcante, F., Fiore, S., Piccarreta, G. & Tateo, F. 2003. Geochemical and mineralogical approaches to assessing provenance and deposition of shales: a case study. *Clay Minerals*, **38**, 383–397.

Cawood, P.A. 1986. Stratigraphic and structural relations of the southern Dun Mountain Ophiolite Belt and enclosing strata, northwestern Southland, New Zealand. *New Zealand Journal of Geology and Geophysics*, **29**, 179–203.

Cawood, P.A. 1987. Stratigraphic and structural relations of strata enclosing the Dun Mountain ophiolite belt in the Arthurton–Clinton region, Southland, New Zealand. *New Zealand Journal of Geology and Geophysics*, **30**, 19–36.

Chamley, H. 1989. *Clay Sedimentology*. Springer, Berlin.

Chumakov, N.M. & Zharkov, M.A. 2003. Climate during the Permian–Triassic Biosphere Reorganizations. Article 2. Climate of the Late Permian and Early Triassic: general Inferences. *Stratigraphy and Geological Correlation*, **11**, 361–375.

Condie, K.C. 1993. Chemical composition and evolution of the upper continental crust: contrasting results from surface samples and shales. *Chemical Geology*, **104**, 1–37.

Coombs, D.S., Landis, C.A., Norris, R.J., Sinton, J.M., Borns, D.J. & Craw, D. 1976. The Dun Mountain ophiolite belt, New Zealand, its tectonic setting, constitution and origin, with special reference to the southern portion. *American Journal of Science*, **276**, 561–603.

Cox, R., Lowe, D.R. & Cullers, R.L. 1995. The influence of sediment recycling and basement composition on evolution of mudrock chemistry in the southwestern United States. *Geochimica et Cosmochimica Acta*, **59**, 2919–2940.

Craw, D. 1979. Melanges and associated rocks, Livingstone Mountains, Southland, New Zealand. *New Zealand Journal of Geology and Geophysics*, **22**, 443–454.

Cronan, D.S. 1976. Basal metalliferous sediments from the eastern Pacific. *Geological Society of America Bulletin*, **87**, 928–934.

Cullers, R.L. 2000. The geochemistry of shales, siltstones and sandstones of Pennsylvanian-Permian age, Colorado, USA: implications for provenance and metamorphic studies. *Lithos*, **51**, 181–203.

Cusker, R.B., Von Dreele, Cox, D.E. & Louër Scardi, P. 1999. Rietveld refinement guidelines. *Journal of Applied Crystallography*, **32**, 36–50.

Davis, T.E., Johnston, M.R., Rankin, P.C. & Stull, R.J. 1980. The Dun Mountain ophiolite belt in east Nelson. *In*: Panayiotou, A. (ed.) *Ophiolites. Proceedings of the International Ophiolite Symposium, Cyprus, 1979*. Cyprus Geological Survey, Nicosia, 480–496.

Dickins, J.M., Johnston, M.R., Kimbrough, D.L. & Landis, C.A. 1986. The stratigraphic and structural position age of the Croisilles Mélange, East Nelson, New Zealand. *New Zealand Journal of Geology and Geophysics*, **29**, 291–301.

Ehrenberg, S.N., Aagaard, P., Wilson, M.J., Fraser, A.R. & Duthie, D.M.L. 1993. Depth-dependent transformation of kaolinite to dickite in sandstones of the Norwegian Continental shelf. *Clay Minerals*, **28**, 325–352.

Ejeh, O.I. 2016. Geochemical discriminant for provenance characterization and palaeogeography of shales from Dahomey Embayment, Southwestern Nigeria. *Journal of Geoscience and Environment Protection*, **4**, 56–68.

Erwin, D.H. 1993. *The Great Paleozoic Crisis: Life and Death in the Permian*. Columbia University Press, New York.

Fedo, C.M., Nesbitt, H.W. & Young, G.M. 1995. Unravelling the effects of potassium metasomatism in sedimentary rocks and paleosols, with implications for paleoweathering conditions and provenance. *Geology*, **23**, 921–924.

Fitton, J.G., Saunders, A.D., Larsen, L.M., Hardarson, B. & Norry, M.J. 1998. Volcanic rocks from the southeast Greenland margin at 63°N: Composition, petrogenesis and mantle sources. *In*: Saunders, A.D., Larsen, H.C. & Wise, S.W., Jr. (eds) *Proceedings of the Ocean Drilling Program Scientific Results*, **152**. International Ocean Discovery Program, College Station, TX, 331–350.

Galfetti, T., Bucher, H. *et al.* 2007. Timing of the Early Triassic carbon cycle perturbations inferred from new U–Pb ages and ammonoid biochronozones. *Earth and Planetary Science Letters*, **258**, 593–604.

Girty, G.H., Ridge, D.L., Knaack, C., Johnson, G. & Al-Riyami, R.K. 1996. Provenance and depositional setting of Paleozoic chert and argillite, Sierra Nevada, California. *Journal of Sedimentary Research*, **66**, 107–118.

Golonka, J. & Ford, D. 2000. Pangean (late Carboniferous–Middle Jurassic) paleoenvironment and lithofacies. *Palaeogeography, Palaeoclimatology, Palaeoecology*, **161**, 1–34.

Gradstein, F.M., Ogg, J.G., Schmitz, M.D. & Ogg, G.M. 2012. *The Geologic Time Scale 2012*. Elsevier, Oxford.

Gromet, L.P., Dymelk, R.F., Haskin, L.A. & Korotev, R.L. 1984. The 'North American Shale Composite': its composition, major and trace element characteristics. *Geochimica et Cosmochimica Acta*, **48**, 2469–2482.

Gu, X.X., Liu, J.M., Zheng, M.H., Tang, J.X. & Qi, L. 2002. Provenance and tectonic setting of the Proterozoic turbidites in Hunan, South China: geochemical evidence. *Journal of Sedimentary Research*, **72**, 393–407.

Haskin, L.A., Frey, F.A. & Wildeman, T.R. 1968. Relative and absolute terrestrial abundances of the rare earths. *In*: Ahrens, L.A. (ed.) *Origin and Distribution of the Elements*. Pergamon Press, 889–912.

Hassan, S., Ishiga, H., Roser, B.P., Dozen, K. & Naka, T. 1999. Geochemistry of Permian–Triassic shales in the Salt Range, Pakistan: implications for provenance and tectonism at the Gondwana margin. *Chemical Geology*, **158**, 293–314.

Hayashi, K.-I., Fujisawa, H., Holland, H.D. & Ohmoto, H. 1997. Geochemistry of *c.* 1.9 Ga sedimentary rocks from northeastern Labrador, Canada. *Geochimica et Cosmochimica Acta*, **61**, 4115–4137.

Herron, M.M. 1988. Geochemical classification of terrigenous sands and shales from core or log data. *Journal of Sedimentary Petrology*, **58**, 820–829.

Joachimski, M.M., Lai, X. *et al.* 2012. Climate warming in the latest Permian and the Permian–Triassic mass extinction. *Geology*, **40**, 195–198.

Johnston, M.R. 1981. *Geological Map of New Zealand 1:50 000, Sheet O27AC – Dun Mountain*. Department of Scientific and Industrial Research, Wellington.

Johnston, M.R. 1982. *Geological Map of New Zealand, 1:50 000, Sheet N28 BD, Red Hills*. Department of Scientific and Industrial Research, Wellington.

Johnston, M.R. 2011. Pakohe – a rock that sustained early Maori society in New Zealand. *In*: Ortiz, J.E., Puche, O., Rabaio, I. & Muadtego, L.F. (eds) *History of Research in Mineral Resources*. Cuadernos del Mutco Geominero, **3**. Instituía Geológico y Minero de España, Madrid, **13**, 61–74.

Jugum, D. 2009. *A tectonic synthesis of the Dun Mountain Ophiolite Belt*. PhD thesis, University of Otago, Dunedin, New Zealand.

Jugum, D., Stewart, E., Palin, J.M., Mortimer, N., Norris, R.J. & Lamb, W.M. 2019. Correlations between a heterogeneous mantle and multiple stages of crustal growth: a review of the Dun Mountain ophiolite, New Zealand. *In*: Robertson, A.H.F. (ed.) *Paleozoic–Mesozoic Geology of South Island, New Zealand: Subduction-related Processes Adjacent to SE Gondwana*. Geological Society, London, Memoirs, **49**, 75–92, https://doi.org/10.1144/M49.3

Kasanzu, C., Maboko, M.A.H. & Manya, S. 2008. Geochemistry of fine-grained clastic sedimentary rocks of the Neoproterozoic Ikorongo Group, NE Tanzania: implications for provenance and source rock weathering. *Precambrian Research*, **164**, 201–213.

Kimbrough, D.L., Mattinson, J.M., Coombs, D.S., Landis, C.A. & Johnston, M.R. 1992. Uranium–lead ages from the Dun Mountain Ophiolite Belt and Brook Street Terranes, South Island, New Zealand. *Geological Society of America Bulletin*, **104**, 429–443.

Krull, E.S., Retallack, G.J., Campbell, H.J. & Lyon, G.L. 2000. $\delta^{13}C$(org) chemostratigraphy of the Permian–Triassic boundary in the Maitai Group, New Zealand: evidence for high latitudinal

methane release. *New Zealand Journal of Geology and Geophysics*, **43**, 21–32.

Landis, C.A. 1969. *Upper Permian rocks of South Island, New Zealand: lithology, stratigraphy, structure, metamorphism and tectonics*. PhD thesis, University of Otago, Dunedin, New Zealand.

Landis, C.A. 1974. Stratigraphy, lithology, structure and metamorphism of Permian, Triassic and Tertiary rocks between the Mararoa River and Mount Snowdon, western Southland, New Zealand. *Journal of the Royal Society of New Zealand*, **4**, 229–251.

Landis, C.A. 1980. Little Ben Sandstone, Maitai Group (Permian): nature and extent in the Hollyford–Eglinton region, South Island, New Zealand. *New Zealand Journal of Geology and Geophysics*, **23**, 551–567.

Landis, C.A. & Blake, M.C., Jr. 1987. Tectonostratigraphic terranes of the Croisilles Harbour region, South Island, New Zealand. *In*: Leitch, E.C. & Scheibner, E. (eds) *Terrane Accretion and Orogenic Belts*. American Geophysical Union, Geodynamics Series, **19**, 179–198.

Le Maitre, R.W. 1976. The chemical variability of some common igneous rocks. *Journal of Petrology*, **17**, 589–598.

Lee, Y.I. 2002. Provenance derived from the geochemistry of late Paleozoic–early Mesozoic mudrocks of the Pyeongan Supergroup, Korea. *Sedimentary Geology*, **149**, 219–235.

Long, X., Sun, M., Yuan, C., Xiao, W. & Cai, K. 2008. Early Paleozoic sedimentary record of the Chinese Altai: implications for its tectonic evolution. *Sedimentary Geology*, **208**, 88–100.

Manikyamba, C., Kerrich, R., González-Álvarez, I., Mathur, R. & Khanna, T.C. 2008. Geochemistry of Paleoproterozoic black shales from the Intracontinental Cuddapah basin, India: implications for provenance, tectonic setting, and weathering intensity. *Precambrian Research*, **162**, 424–440.

McCoy-West, A.J., Mortimer, N. & Ireland, T.R. 2014. U–Pb geochronology of Permian plutonic rocks, Longwood Range, New Zealand: implications for Median Batholith–Brook Street Terrane relations. *New Zealand Journal of Geology and Geophysics*, **57**, 65–85.

McLennan, S.M. 1989. Rare earth elements in sedimentary rocks: influence of provenance and sedimentary processes. *In*: Lipin, B.R. & McKay, G.A. (eds) *Geochemistry and Mineralogy of Rare Earth Elements*. Mineralogical Society of America, Reviews in Mineralogy, **21**, 169–200.

McLennan, S.M., Hemming, S., McDaniel, D.K. & Hanson, G.N. 1993. Geochemical approaches to sedimentation, provenance and tectonics. *In*: Johnsson, M.J. & Basu, A. (eds) *Processes Controlling the Composition of Clastic Sediments*. Geological Society of America, Special Papers, **284**, 21–40.

Miall, A.D. 2013. *Principles of Sedimentary Basin Analysis*. 3rd edn. Springer, New York.

Mortimer, N., Tulloch, A.J., Spark, R.N., Walker, N.W., Ladley, E., Allibone, A. & Kimbrough, D.L. 1999. Overview of the Median Batholith, New Zealand: a new interpretation of the geology of the Median Tectonic Zone and adjacent rocks. *Journal of African Earth Sciences*, **29**, 257–268.

Mortimer, N., Rattenbury, M.S. *et al.* 2014. High-level stratigraphic scheme for New Zealand rocks. *New Zealand Journal of Geology and Geophysics*, **57**, 402–419.

Muir, R.J., Ireland, T.R., Weaver, S.D., Bradshaw, J.D., Evans, J.A., Eby, G.N. & Shelley, D. 1998. Geochronology and geochemistry of a Mesozoic magmatic arc system, Fiordland, New Zealand. *Journal of the Geological Society, London*, **155**, 1037–1053, https://doi.org/10.1144/gsjgs.155.6.1037

Mullins, E.K. & Weis, D. 2015. Evidence for trench-parallel mantle flow in the northern Cascade Arc from basalt geochemistry. *Earth and Planetary Science Letters*, **414**, 100–107.

Nesbitt, H.W. & Young, G.M. 1982. Early Proterozoic climates and plate motions inferred from major element chemistry of lutites. *Nature*, **299**, 715–717.

Owen, S.R. 1995. *Maitai and Murihiku (Permian and Triassic) rocks in Nelson, New Zealand*. PhD thesis, University of Otago, Dunedin, New Zealand.

Paikaray, S., Banerjee, S. & Mukherji, S. 2008. Geochemistry of shales from the Paleoproterozoic to Neoproterozoic Vindhyan Supergroup: implications on provenance, tectonics and paleoweathering. *Journal of Asian Earth Sciences*, **32**, 34–48.

Paull, R.K., Campbell, J.D. & Coombs, D.S. 1996. New information on the age and thermal history of a probable Early Triassic siltstone near Kaka Point, South Island. *New Zealand*, **39**, 581–584.

Pillai, D.D.L. 1989. *Upukerora Formation, Maitai Group, in western Otago and northern Southland*. MSc thesis, University of Otago, Dunedin, New Zealand.

Potter, P.E., Maynard, J.B. & Depetris, P.J. 2005. *Mud and Mudstones: Introduction and Overview*. Springer, Heidelberg.

Price, R.C., Ireland, T.R., Maas, R. & Arculus, R.J. 2006. SHRIMP ion probe zircon geochronology and Sr and Nd isotope geochemistry for southern Longwood Range and Bluff Peninsula intrusive rocks of Southland, New Zealand. *New Zealand Journal of Geology and Geophysics*, **49**, 291–303.

Price, R.C., Spandler, C.J., Arculus, R.J. & Reay, A. 2011. The Longwood Igneous Complex, Southland, New Zealand: a Permo-Jurassic, intra-oceanic, subduction-related, I-type batholithic complex. *Lithos*, **126**, 1–21.

Raine, J.I., Beu, A.G. *et al.* 2015. New Zealand Geological Timescale NZGT 2015/1. *New Zealand Journal of Geology and Geophysics*, **58**, 398–403.

Rattenbury, M.S., Cooper, R.A. & Johnston, M.R. (compilers) 1998. *Geology of the Nelson Area. 1:250 000*. Institute of Geological and Nuclear Sciences Geological Map, **9**. Institute of Geological and Nuclear Sciences Limited, Lower Hutt, New Zealand.

Renne, P.R., Zichao, Z., Richards, M.A., Black, M.T. & Basu, R.T. 1995. Synchrony and causal relations between Permian–Triassic boundary crises and Siberian flood volcanism. *Science*, **269**, 1413–1416.

Retallack, G.J. 1999. Post-apocalyptic greenhouse paleoclimate revealed by earliest Triassic paleosols in the Sydney Basin, Australia. *Geological Society of America Bulletin*, **111**, 52–70.

Retallack, G.J. & Krull, E.S. 1999. Landscape ecological shift at the Permian–Triassic boundary in Antarctica. *Australian Journal of Earth Sciences*, **46**, 785–812.

Robertson, A.H.F. 2019*a*. Patuki and Croisilles melanges in South Island, New Zealand: genesis related to Permian subduction–accretion processes. *In*: Robertson, A.H.F. (ed.) *Paleozoic–Mesozoic Geology of South Island, New Zealand: Subduction-related Processes Adjacent to SE Gondwana*. Geological Society, London, Memoirs, **49**, 119–156, https://doi.org/10.1144/M49.10

Robertson, A.H.F. 2019*b*. Mid–Late Permian Upukerora Formation, South Island, New Zealand: fault-controlled mass wasting of the Permian Dun Mountain ophiolite and initiation of the Permian–Triassic Maitai continental margin forearc basin. *In*: Robertson, A.H.F. (ed.) *Paleozoic–Mesozoic Geology of South Island, New Zealand: Subduction-related Processes Adjacent to SE Gondwana*. Geological Society, London, Memoirs, **49**, 157–188, https://doi.org/10.1144/M49.12

Robertson, A.H.F. & Palamakumbura, R. 2019*a*. Geological development and regional significance of an oceanic magmatic arc and its sedimentary cover: Permian Brook Street Terrane, South Island, New Zealand. *In*: Robertson, A.H.F. (ed.) *Paleozoic–Mesozoic Geology of South Island, New Zealand: Subduction-related Processes Adjacent to SE Gondwana*. Geological Society, London, Memoirs, **49**, 43–73, https://doi.org/10.1144/M49.11

Robertson, A.H.F. & Palamakumbura, R. 2019*b*. Sedimentary development of the Mid-Permian–Mid-Triassic Maitai continental margin forearc basin, South Island, New Zealand. *In*: Robertson, A.H.F. (ed.) *Paleozoic–Mesozoic Geology of South Island, New Zealand: Subduction-related Processes Adjacent to SE Gondwana*. Geological Society, London, Memoirs, **49**, 189–230, https://doi.org/10.1144/M49.9

Robertson, A.H.F. & Palamakumbura, R. 2019*c*. Sedimentary geochemistry used to infer the provenance of Permian–Triassic marine sandstones related to the SE Gondwana active continental

margin, South Island, New Zealand. *In*: Robertson, A.H.F. (ed.) *Paleozoic–Mesozoic Geology of South Island, New Zealand: Subduction-related Processes Adjacent to SE Gondwana*. Geological Society, London, Memoirs, **49**, 231–265, https://doi.org/10.1144/M49.14

Robertson, A.H.F. & Sharp, T.R. 2002. Geochemical and mineralogical evidence for the provenance of mixed volcanogenic/terrigenous hemipelagic sediments in the Pliocene–Pleistocene Woodlark backarc rift basin, southwest Pacific: Ocean Drilling Program Leg 180. *In*: Huchon, P., Taylor, B. & Klaus, A. (eds) *Proceedings of the ODP, Scientific Results*, **180**. Ocean Drilling Program, College Station, TX, http://www.odp.tamu.edu/publications/180_SR/156/156.htm

Robertson, A.H.F., Campbell, H.J., Johnston, M.R. & Palamakumbura, R. 2019*a*. Construction of a Paleozoic–Mesozoic accretionary orogen along the active continental margin of SE Gondwana (South Island, New Zealand): summary and overview. *In*: Robertson, A.H.F. (ed.) *Paleozoic–Mesozoic Geology of South Island, New Zealand: Subduction-related Processes Adjacent to SE Gondwana*. Geological Society, London, Memoirs, **49**, 331–372, https://doi.org/10.1144/M49.8

Robertson, A.H.F., Campbell, H.J., Johnston, M.R. & Mortimer, N. 2019*b*. Introduction to Paleozoic–Mesozoic geology of South Island, New Zealand: subduction-related processes adjacent to SE Gondwana. *In*: Robertson, A.H.F. (ed.) *Paleozoic–Mesozoic Geology of South Island, New Zealand: Subduction-related Processes Adjacent to SE Gondwana*. Geological Society, London, Memoirs, **49**, 1–14, https://doi.org/10.1144/M49.7

Robertson, A.H.F., Palamakumbura, R.N. & Campbell, H.J. 2019*c*. Permian–Triassic felsic tuffs in South Island, New Zealand: significance for oceanic and active continental margin subduction. *In*: Robertson, A.H.F. (ed.) *Paleozoic–Mesozoic Geology of South Island, New Zealand: Subduction-related Processes Adjacent to SE Gondwana*. Geological Society, London, Memoirs, **49**, 293–321, https://doi.org/10.1144/M49.15

Rollinson, H.R. 1993. *Using Geochemical Data: Evaluation, Presentation, Interpretation*. Longman, London.

Roser, B.P. & Korsch, R.J. 1986. Determination of tectonic setting of sandstone–mudstone suites using SiO_2 content and K_2O/Na_2O ratio. *Journal of Geology*, **94**, 635–650.

Roser, B.P. & Korsch, R.J. 1988. Provenance signatures of sandstone–mudstone suites determined using discriminant function analysis of major element data. *Chemical Geology*, **67**, 119–139.

Sayles, F.L. & Bischoff, J.L. 1973. Ferromanganoan sediments in the equatorial East Pacific. *Earth and Planetary Science Letters*, **19**, 330–336.

Sinton, J.M. 1980. Petrology and evolution of the Red Mountain Ophiolite Complex, New Zealand. *American Journal of Science*, **280**, 296–328.

Sivell, W.J. 2002. Geochemistry and Nd-isotope systematics of chemical and terrigenous sediments from the Dun Mountain Ophiolite, New Zealand. *New Zealand Journal of Geology and Geophysics*, **45**, 427–451.

Sivell, W.J. & McCulloch, M.T. 2000. Reassessment of the origin of the Dun Mountain Ophiolite, New Zealand: Nd-isotopic and geochemical evolution of magma suites. *New Zealand Journal of Geology and Geophysics*, **43**, 133–146.

Stratford, J.M.C., Landis, C.A., Owen, S.R., Gilmour, E.H., McCulloch, M.E. & Campbell, H.J. 2004. Stratigraphy of the lower Maitai Group at West Dome, southland, New Zealand. *Journal of the Royal Society of New Zealand*, **34**, 267–293.

Sun, S.-S. & McDonough, W.F. 1989. Chemical and isotopic systematics of ocean basalts: implications for mantle composition and processes. *In*: Saunders, A.D. & Norry, M.J. (eds) *Magmatism in the Ocean Basins*. Geological Society, London, Special Publications, **42**, 313–345, https://doi.org/10.1144/GSL.SP.1989.042.01.19

Swain, G., Barovich, K., Hand, M., Ferris, G. & Schwarz, M. 2008. Petrogenesis of the St Peter Suite, southern Australia: arc magmatism and Proterozoic crustal growth of the South Australian Craton. *Precambrian Research*, **166**, 283–296.

Taylor, S.R. & McLennan, S.M. 1985. *The Continental Crust: Its Composition and Evolution*. Blackwell, Oxford.

Taylor, R.N. & Nesbitt, R.W. 1998. Isotopic characteristics of subduction fluids in an intra-oceanic setting, Izu-Bonin arc, Japan. *Earth and Planetary Science Letters*, **164**, 79–98.

Tucker, M.E. 1991. *Sedimentary Petrology. An Introduction to the Origin of Sedimentary Rocks*. 2nd edn. Blackwell, Oxford.

Turnbull, I.M. (compiler) 2000. *Geology of the Wakatipu Area. 1:250 000*. Institute of Geological and Nuclear Sciences Geological Map, **18**. Institute of Geological and Nuclear Sciences Limited, Lower Hutt, New Zealand.

Turnbull, I.M. & Allibone, A.H. (compilers) 2003. *Geology of the Murihiku Area. 1:250 000*. Institute of Geological and Nuclear Sciences Geological Map, **20**. Institute of Geological and Nuclear Sciences Limited, Lower Hutt, New Zealand.

Veevers, J.J. 1990. Tectonic–climatic super cycle in the billion-year plate-tectonic eon: Permian Pangean icehouse alternates with Cretaceous dispersed-continents greenhouse. *Sedimentary Geology*, **68**, 1–16.

Walker, J.R. 1991. Chlorite polytypism – a possible geothermometer? *In*: *Program and Abstracts for Clay Minerals Society, 28th Annual Meeting. 5–10 October 1991, Houston, TX*. Lunar & Planetary Institute, Houston, TX, 164.

Waterhouse, J.B. 1959. Stratigraphy of the lower part of the Maitai Group, Nelson. *New Zealand Journal of Geology and Geophysics*, **2**, 944–953.

Waterhouse, J.B. 1964. *Permian Stratigraphy and Faunas of New Zealand*. New Zealand Geological Survey Bulletin, **72**.

Waterhouse, J.B. 1980. Permian bivalves of New Zealand. *Journal of the Royal Society of New Zealand*, **10**, 97–133.

Wronkiewicz, J. & Condie, C. 1987. Geochemistry of Archean shales from the Witwatersrand Supergroup, South Africa: source-area weathering and provenance. *Geochimica et Cosmochima Acta*, **51**, 2401–2416.

Yan, Z., Wang, Z., Yan, Q., Wang, T. & Guo, X. 2012. Geochemical constraints on the provenance and depositional setting of the Devonian Liuling Group, east Qinling Mountains, Central China: Implications for the tectonic evolution of the Qinling orogenic belt. *Journal of Sedimentary Research*, **82**, 9–20.

Yang, X.F., He, D.F., Wang, Q.C., Tang, Y., Tao, H.F. & Li, D. 2012. Provenance and tectonic setting of the Carboniferous sedimentary rocks of the East Junggar Basin, China: evidence from geochemistry and U–Pb zircon geochronology. *Gondwana Research*, **22**, 567–584.